A storm safari in Subtropical South America:



proyecto RELAMPAGO

- 3 Stephen W. Nesbitt¹, Paola V. Salio², Eldo Ávila³, Phillip Bitzer⁴, Lawrence Carey⁴, V.
- 4 Chandrasekar⁵, Wiebke Deierling⁶⁷, Francina Dominguez¹, Maria Eugenia Dillon⁸⁹, C.
- 5 Marcelo Garcia¹⁰, David Gochis⁷, Steven Goodman¹¹, Deanna A. Hence¹, Karen A. Kosiba¹²,
- 6 Matthew R. Kumjian¹³, Timothy Lang¹⁴, Lorena Medina Luna⁷, James Marquis¹⁵, Robert
- 7 Marshall⁶, Lynn A. McMurdie¹⁶, Ernani Lima Nascimento¹⁷, Kristen L. Rasmussen⁵, Rita
- 8 Roberts⁷, Angela K. Rowe¹⁸, Juan José Ruiz², Eliah F.M.T. São Sabbas¹⁹, A. Celeste Saulo^{8 9},
- 9 Russ S. Schumacher⁵, Yanina Garcia Skabar⁸, Luiz Augusto Toledo Machado¹⁹, Robert J.
- 10 Trapp¹, Adam Varble¹⁵, James Wilson⁷, Joshua Wurman¹², Edward J. Zipser²⁰, Ivan Arias⁵,
- 11 Hernán Bechis² and Maxwell A. Grover¹
- 13 ¹Department of Atmospheric Sciences, University of Illinois at Urbana-Champaign, Illinois,
- 14 *USA*.

12

1

2

- ²Centro de Investigaciones del Mar y la Atmósfera, CONICET-UBA. Departamento de
- 16 Ciencias de la Atmósfera y los Océanos, UBA, UMI-IFAECI, CNRS-CONICET-UBA, Buenos
- 17 Aires, Argentina.
- 18 ³Facultad de Matemática, Astronomía, Física y Computación, Universidad Nacional de
- 19 Córdoba. Instituto de Física Enrique Gaviola, CONICET, Córdoba, Argentina.
- 20 ⁴Atmospheric Science Department, University of Alabama, Huntsville, Alabama, USA.
- ⁵Colorado State University, Fort Collins, Colorado, USA.
- 22 ⁶Aerospace Engineering Sciences Department, University of Colorado Boulder, Boulder,
- 23 Colorado, USA

1

Early Online Release: This preliminary version has been accepted for publication in *Bulletin of the American Meteorological Society*, may be fully cited, and has been assigned DOI 10.1175/BAMS-D-20-0029.1. The final typeset copyedited article will replace the EOR at the above DOI when it is published.

- ⁷National Center for Atmospheric Research, Boulder, Colorado, USA.
- 25 ⁸Servicio Meteorológico Nacional, Buenos Aires, Argentina
- ⁹Comité Nacional de Investigaciones Científicas y Técnicas, Argentina.
- 27 ¹⁰Facultad de Ciencias Exactas, Físicas y Naturales, Universidad Nacional de Córdoba,
- 28 Córdoba, Argentina.
- 29 ¹¹Thunderbolt Global Analytics, Huntsville, AL, USA.
- 30 ¹²Center for Severe Weather Research, Boulder, Colorado, USA.
- 31 ¹³Department of Meteorology and Atmospheric Science, The Pennsylvania State University,
- 32 University Park, Pennsylvania, USA.
- 33 ¹⁴NASA Marshall Space Flight Center Huntsville, Alabama, USA.
- 34 ¹⁵Pacific Northwest National Laboratory, Richland, Washington, USA.
- 35 ¹⁶Department of Atmospheric Sciences, University of Washington, Seattle, Washington, USA.
- 36 ¹⁷Universidade Federal de Santa Maria, Santa Maria, Brazil.
- 37 ¹⁸Department of Atmospheric and Oceanic Sciences, University of Wisconsin-Madison,
- 38 Madison, WI, USA.
- 39 ¹⁹Instituto Nacional de Pesquisas Espaciais, São José dos Campos, Brazil
- 40 ²⁰University of Utah, Salt Lake City, Utah, USA.
- Submitted to the Bulletin of the American Meteorological Society
- 42 Revised 4 April 2021
- 43 Corresponding author: Stephen W. Nesbitt, Department of Atmospheric Sciences, University
- of Illinois at Urbana-Champaign, 1301 W. Green St., Urbana, IL 61801 snesbitt@illinois.edu

45 ABSTRACT

This article provides an overview of the experimental design, execution, education and
public outreach, data collection, and initial scientific results from the Remote sensing of
Electrification, Lightning, And Mesoscale/microscale Processes with Adaptive Ground
Observations (RELAMPAGO) field campaign. RELAMPAGO was a major field campaign
conducted in Córdoba and Mendoza provinces in Argentina, and western Rio Grande do Sul
State in Brazil in 2018-2019 that involved more than 200 scientists and students from the US
Argentina, and Brazil. This campaign was motivated by the physical processes and societal
impacts of deep convection that frequently initiates in this region, often along the complex
terrain of the Sierras de Córdoba and Andes, and often grows rapidly upscale into dangerous
storms that impact society. Observed storms during the experiment produced copious hail,
intense flash flooding, extreme lightning flash rates and other unusual lightning phenomena,
but few tornadoes. The 5 distinct scientific foci of RELAMPAGO: convection initiation,
severe weather, upscale growth, hydrometeorology, and lightning and electrification are
described, as are the deployment strategies to observe physical processes relevant to these
foci. The campaign's international cooperation, forecasting efforts, and mission planning
strategies enabled a successful data collection effort. In addition, the legacy of
RELAMPAGO in South America, including extensive multi-national education, public
outreach, and social media data-gathering associated with the campaign, is summarized.
CAPSULE (BAMS ONLY)
RELAMPAGO was a multinational field campaign that collected detailed measurements
of deep convective storms, high-impact weather, and their effects in Argentina and Brazil.

1. Introduction

68

69

70

71

72

73

74

75

76

77

78

79

80

81

82

83

84

85

86

87

88

89

90

The United States (US) is infamous for its hazardous convective storms that produce high-impact weather (HIW), including tornadoes, hail, strong winds, lightning, heavy precipitation, and flooding, and cause significant loss of life and property. The hazardous storms are also important components of the regional climate over much of the eastern twothirds US. Past field campaigns, observational studies, and model experiments have produced knowledge that is the foundation of current forecast capabilities of hazardous weatherproducing storms in the US. Much of this knowledge was gained from storms studied over the US Great Plains region (e.g., Rasmussen et al. 1994; Davis et al. 2004; Wurman et al. 2012; Geerts et al. 2017). Studies of Great Plains severe thunderstorms link their occurrence and hazards to abundant lower-tropospheric moisture, steep mid-tropospheric lapse rates, and strong tropospheric vertical wind shear (e.g., Doswell et al. 1996). The specific presence of tornadoes is additionally linked to strong lower tropospheric vertical wind shear (e.g., Thompson et al. 2012). In contrast to the US, where these ingredients and resultant storms have been extensively studied, in other regions of the world, severe weather and its ingredients may or may not follow the "template" of storms in the US. While severe convective storms in Europe have garnered recent study (e.g., Groenemeijer et al. 2017), the recognition of other intense, organized convective hotspots enabled by spaceborne radar – including Southeast South America (SESA), central Africa, and the Indian Subcontinent (Nesbitt et al. 2006; Zipser et al. 2006; Houze et al. 2015) have not been accompanied by extensive in situ and surface-based remote sensing studies of convective storm evolution and

lifecycle similar to those conducted in the US and Europe.

Severe weather is reported in many satellite-identified global convective hotspots (Bang
and Cecil 2019), However, differently configured meteorological services and inconsistent
severe weather databases outside the US make the use of event reports challenging in
comparing among various regions of the world. Even in the US, forecasting and nowcasting
severe convection remains challenging (e.g., Herman et al. 2018; Brooks and Correia 2018),
and there is significant uncertainty in predicting how the frequency and nature of convective
storms may change in the future (National Academy of Sciences, Medicine, and Engineering
2016). With a goal of improving the understanding of global severe convective storms, we
are motivated by the following questions: To what extent do the meteorological and
geographical ingredients for severe convective storms in intense convective hotspots, often
patterned after storms in North America, translate across the globe? Are the hazards
associated with archetypical storms and their environments (i.e., supercells, mesoscale
convective systems, multicell storms), and conceptual models of storm lifecycle and lifecycle
transitions and their associated hazard probabilities generated from US storms consistent
across global regions? How do proxies for severe storm frequency from satellites and large-
scale models compare with detailed observations in severe storms, particularly in regions
where the physical processes producing severe weather may differ?

The answers to these questions ultimately impact our ability to monitor and predict severe convective hazards globally on both weather and climate timescales, as well as using statistical techniques that relate storm environments to hazards (e.g., Trapp et al. 2007). We postulate that the answers to these questions through intensive field observations and modeling efforts the global convective hotspots can help to provide the answers to these, and other questions that currently limit predictability of severe storms both globally – and over the US – by revealing new insights into the physical processes in convective storms, as well

as anticipate changes in global convective hazard frequency and intensity under potential future climate change scenarios.

SESA has unique meteorological conditions and geography compared with the US Great Plains that results in a high spatial density of convective storms in a variety of storm modes that form in the lee of unique continental-scale and mesoscale topography (Rasmussen and Houze 2016; Mulholland et al. 2018). SESA also has a relatively long convective season (austral spring through autumn; Zipser et al. 2006; Rasmussen and Houze 2011), and terrain-focused convective initiation regions (Cancelada et al. 2020) making it an ideal natural laboratory to study the initiation and evolution of deep convection, the role of complex terrain in modulating convective processes, and attendant HIW using fixed and mobile observatories. Motivated by the scientific questions identified above, along with further scientific rationale described below, the Remote sensing of Electrification, Lightning, And Mesoscale/microscale Processes with Adaptive Ground Observations (RELAMPAGO) field campaign was conducted to study the HIW producing storms in this region.

(a) An intense convection hotspot

RELAMPAGO observed the unique environmental and storm processes in central Argentina, where the convective systems, according to satellite-based analysis, contains superlative convective structures by many measures. Satellite-based tracking of mesoscale convective systems (MCSs) formed near the Andes, and the Sierras de Córdoba (SDC), a prominent mesoscale mountain range located roughly 700 km to the east of the Andes, have revealed their extreme size and propagation to regions as far away as Bolivia and coastal Brazil (Velasco and Fritsch 1987; Durkee et al. 2009; Vidal 2014). In SESA, MCSs contribute 90% or more of the annual rainfall and contain extremely deep and wide convective cores (Nesbitt et al. 2006; Houze et al. 2015; Rasmussen et al. 2016), which make

this region prone to extreme rainfall and flash and riverine flooding (Hamada et al. 2015).
The most vertically extensive radar echo observed by satellite precipitation radar (Zipser et
al. 2006) occurred in central Argentina, and the region features the highest frequency of low
microwave brightness temperatures as a proxy for hail frequency (Cecil and Blankenship
2012; Bang and Cecil 2019) as well as the highest lightning flash counts per storm (Cecil et
al. 2005; Zipser et al. 2006). The NOAA GOES-16 Geostationary Lightning Mapper
observed the most extensive (>700 km, 31 October 2018) and longest duration (16.73 s, 4
March 2019) World Meteorological Organization-record lightning flashes in Argentina
(Petersen et al. 2020). Satellite and ground-based radar observations indicate that the storm
modes in the region near the SDC can produce supercells quickly after orogenic convection
initiation (CI), which can grow upscale into MCSs much more rapidly than in the US Great
Plains (Mulholland et al. 2018). In contrast to the US, a large number of SESA convective
systems appear to backbuild (e.g., Schumacher 2015; Peters and Schumacher 2015) with
respect to the mid- and upper-level flow, with new updrafts developing on the upstream
(west) side of the storm (Anabor et al. 2008, 2009; Rasmussen et al. 2014).
The region near the SDC commonly experiences severe hail (Mezher et al 2012; Matsudo
and Salio 2011; Rasmussen et al. 2014), with hailstones even reaching gargantuan sizes
(Kumjian et al. 2021). Farther west, near the Andes, is the Mendoza region, which is
infamous for its frequency of damaging hailstorms; 8% of days between 15 October and 31
March between 2000 and 2003 observed hail >2 cm (Rosenfeld et al. 2006). Tornadoes are
also observed in central Argentina, but the regions of observed maximum tornado frequency
are located well east of the SDC, and are rarely observed near the SDC or Andes (Altinger de
Schwarzkopf and Rosso 1982; Brooks and Doswell 2001; Rasmussen et al. 2014) despite the
presence of supercell thunderstorms (Mulholland et al. 2018; Trapp et al. 2020).

(b) Synoptic-scale ingredients

163

164

165

166

167

168

169

170

171

172

173

174

175

176

177

178

179

180

181

182

183

184

185

186

Midlatitude synoptic disturbances in the Southern Hemisphere subtropical jet, and attendant jet streaks, are greatly deformed when they encounter the massive Andes Mountains. The subtropical jet, located near 30°S latitude throughout much of the year, provides for strong deep-layer vertical wind shear and cold air advection aloft, resulting in steep mid-level lapse rates (Ribiero and Bosart 2018). Jet streak-Andes interactions can modulate the low-level flow downstream over Argentina (Shapiro 1981; Rasmussen and Houze 2016). The South American low-level jet (SALLJ) facilitates tropical-extratropical exchange in South America, transporting moisture from the Amazon to the La Plata basin and increasing potential instability (Vera et al. 2006). Between 60-70% of precipitation over SESA comes from moisture of terrestrial origin that is predominantly transported by the SALLJ (van der Ent et al. 2010; Martinez and Dominguez 2014), with moisture transport peaking in austral spring months. The poleward penetration of the SALLJ into SESA (Nicolini et al. 2002) is strongly associated with baroclinic disturbances entering the region from the west (Salio et al. 2002; Marengo et al. 2004; Nicolini and Saulo 2006; Salio et al. 2007; Rasmussen and Houze 2016). This poleward penetration often coincides with the deepening of a lee trough called the Northern Argentinean Low (NAL, Seluchi et al. 2003; Saulo et al. 2004; 2007). The NAL enhances the local pressure gradient force, leading to poleward SALLJ penetration near the Andes, with a wind speed maxima (up to 25 m s⁻¹) at 1-1.5-km altitudes as far south as 35°S (Nicolini and Saulo 2006), typically maximizing at night (Nicolini and Garcia Skabar 2011). The enhancement of the SALLJ and NAL with an upper-level disturbance often increases potential instability, deep (0-8 km) vertical wind shear, and low-level wind veering, providing an environment favorable for organized convection (Salio et al 2007; Borque et al.

2010; Rasmussen and Houze 2016; Mulholland et al. 2018). Terrain, cold fronts, stationary fronts, and outflow boundaries from pre-existing convective systems that impinge on the SALLJ can serve as a mechanism for CI. However, the mechanisms of CI and initial survival, and the upscale growth of convective systems as they move away from their initiation location, often observed near terrain, are not well characterized in SESA, or globally (Banta and Schaaf 1987; Wilson and Mueller 1993; Coniglio et al. 2006).

(c) RELAMPAGO Research Themes

Within the framework of the above science questions and the unique geo-climatic setting of SESA, RELAMPAGO, together with its sister project, the Department of Energy-funded Clouds, Aerosols, Complex Terrain Interactions (CACTI) campaign (see accompanying article by Varble et al. 2021), took an integrated and expansive observational approach to document processes relevant to on the following research themes:

Convective initiation: Determine relevant environmental processes that lead to the initiation of deep convection over and near complex terrain and contrast the mechanisms near the SDC and Andes.

Severe convective storms: Observe processes by which hail, strong winds, and tornadoes are generated in environments close to the Andes and SDC, two regions that offer key meteorological and physical-geographical contrasts to severe storm environments in the US.

Upscale growth of convection: Identify kinematic, thermodynamic, microphysical processes by which deep convection intensifies and grows upscale in the immediate vicinity of complex terrain features, including those that produce extremely tall and/or broad convective systems, and contrast these mechanisms near and apart from topography.

Lightning: Observe lightning, Transient Luminous Events (TLEs) and High Energy

Emissions from Thunderstorms (HEETs), determine their characteristics across the spectrum of convective systems in/near the SDC and Andes, and relate those characteristics to processes in deep convective systems.

Hydrometeorology: Characterize the relationship between land surface fluxes, atmospheric processes, and surface/subsurface hydrologic response in the Carcarañá Basin (a sub-basin of

the La Plata basin that includes the SDC eastern slopes), with a focus on extremes.

2. RELAMPAGO observations

RELAMPAGO (summarized in Table 1) deployed a combination of fixed and mobile assets that leveraged the operational observing networks and focused on locations where convective processes of interest were likely found based on climatological studies.

Extending the analysis of Zipser et al. (2006), TRMM observed precipitation radar (PR) echo tops in the 99.9999th percentile are shown in Fig. 1a, indicating the high observed frequency of extremely tall convective cores in the study region. Our operations regions (Fig. 1b) focused on the regions near and to the east of the SDC mountain crest in Córdoba Province (noted the Córdoba domain) and the Andes west of San Rafael, Mendoza Province (noted the Mendoza domain). An operations center established by the National Center for Atmospheric Research Earth Observing Laboratory (NCAR EOL) in Villa Carlos Paz, in the Córdoba domain, provided a location that enabled the preparation of weather forecasts and coordinated deployment of mobile teams (see related sidebars to learn more about these key elements of RELAMPAGO) to the SDC foothills or nearby plains, or to the Mendoza Domain. The CACTI primary site was located in the Sierras de Córdoba near Villa Yacanto which along with terrain-focused CACTI aircraft operations anchored several RELAMPAGO

232	deployments. A fixed site operated by Brazil was located near Sao Borja, Rio Grande do Sul,
233	Brazil, observed convective systems 800 km to the northeast near the Parana River.
234	RELAMPAGO consisted of three stages of deployment (Fig. 2). During an Extended
235	Observing Period (EOP), which extended 5 June 2018 – 30 April 2019, a network of 30
236	hydrometeorological stations was operated across the Rio Carcaraná basin (see Section 2a for
237	more details). The period of mobile operations in RELAMPAGO was 1 November – 17
238	December 2018, during which targeted observations were directed from the RELAMPAGO
239	operations center at Villa Carlos Paz. The Colorado State University (CSU) C-Band dual-
240	polarization radar and enhanced soundings at Córdoba operated until 31 January 2019 and
241	captured observations of several additional storm events.
242	The observational assets in RELAMPAGO were complimented by operational sounding
243	sites at Córdoba, Mendoza, Santa Rosa, Resistencia, Ezeiza, Uruguaiana, Santa Maria, Porto
244	Alegre, and Foz do Iguaçu, which launched at least twice-daily soundings at 00 and 12 UTC
245	throughout the campaign. Operational radars in the region included the C-Band INVAP S.E.
246	RMA-320 dual-polarization Doppler radar operating at Córdoba (RMA1), and 2 S-Band non-
247	Doppler radars operated by Mendoza Province. Mesonet data and rain gauge data cataloged
248	during RELAMPAGO included sites contributed by agricultural, livestock, and water
249	agencies as well as the private sector in Argentina, southern Brazil, and Uruguay.
250	During the RELAMPAGO operations, fixed and mobile platforms were used to collect
251	observations of the thermodynamic and kinematic environment, storm structures, lightning,
252	precipitation, and land surface states and fluxes. Some of these observations were continuous,
253	while others targeted phenomena during the campaign based on RELAMPAGO forecast
254	operations (Sidebar 1). Many of these instruments are depicted in Fig. 3.
255	(a) Hydrometeorological observations

The hydrometeorological EOP began on 1 June 2018, five months before the IOP and
ended on 30 April 2019. The EOP consisted of a network of 15 10-m towers from NCAR's
Earth Observing Laboratory (EOL) (yellow markers in Fig. 4), which included seven eddy
covariance (EC) towers. In addition, we installed 15 2-m towers from NCAR's Research
Application Laboratory (RAL) (magenta markers in Fig. 4). These towers, installed
throughout a broad region encompassing the SDC and adjacent eastern plains, collected basic
hydrometeorological measurements (temperature, humidity, precipitation, soil moisture, etc.),
and drop size distributions (in addition to a NASA-deployed disdrometer site in Córdoba),
whereas the EC towers measured turbulent energy, moisture, and momentum fluxes. The
EOP was conducted to understand how land surface heterogeneity impacts the initiation and
growth of convection on hydrologically-relevant timescales, and how precipitation is
partitioned into subsurface infiltration, runoff, and evapotranspiration.

During the RELAMPAGO operations, the Hydrometeorology ("Hydromet") team performed streamflow observations along the headwater rivers of the SDC (Fig. 4). Two months prior to the start of mobile operations, eight stream-level sensors were deployed (cyan stars in Fig. 4) and gathered cross-section information. Performing streamflow observations associated with convective events is difficult because of the uncertainty in forecasting the intensity and location of the events, as well as the fast hydrological response of the basins.

Teams were deployed to measure streamflow with Acoustic Doppler Current Profilers and with digital cameras to perform Large Scale Particle Image Velocimetry measurements along the selected river cross-sections. LSPIV, a non-intrusive flow velocimetry technique, quantified streamflow during flash flood events. During RELAMPAGO, the team performed a total of 10 observational campaigns, including several extreme hydrometeorological events on 5, 11-12, and 27 November 2018. Due to the abundance of events, we were able to

construct the stage-discharge curves for the upper basin for the Santa Rosa, Quillinzo and La
 Cruz sites.

(b) Soundings and mobile in situ observations

282

283

284

285

286

287

288

289

290

291

292

293

294

295

296

297

298

299

300

301

302

303

Balloon-borne soundings from fixed and mobile platforms provided an unprecedented view of the environments supporting the initiation, organization, and maintenance of convection in RELAMPAGO. When including data from operational sounding sites and the DOE-ARM site, 2712 soundings were collected during the RELAMPAGO-CACTI EOP. Of these, 1557 were collected during the RELAMPAGO campaign (28 October-18 December 2018), and 574 of these were launched from vehicles that were highly mobile, positioned in targeted locations for each intensive observing period (IOP), sometimes redeployed within an IOP. The Servicio Meteorológico Nacional (SMN) provided 532 soundings at Villa Maria del Río Seco and supplemental soundings at Córdoba, Mendoza and Resistencia (these soundings were uploaded to the Global Telecommunications System). The Center for Severe Weather Research (CSWR) deployed 3 mobile mesonet trucks, measuring wind, temperature, and relative humidity, mounted far forward of the vehicle slipstream at 4 m AGL. CSWR also deployed 15 1-m portable weather stations or "Pods" to targeted locations, measuring temperature, relative humidity, wind velocity, and pressure. The mesonet vehicles typically deployed the Pods to observe transects on available paved roads to measure spatiotemporal variations in storm inflow and outflow.

Schumacher et al. (2020) describes RELAMPAGO sounding operations. Fig. 5 shows a time series of equivalent potential temperature, and *u*- and *v*-wind components from Córdoba including supplemental RELAMPAGO soundings, as well as the timing of RELAMPAGO missions. Periods of enhanced vertical wind shear, enhanced northerly low-level flow associated with the SALLJ, and low-level potential instability coincided with several IOPs,

but not all where deep convection was observed. In all, the bulk of RELAMPAGO sounding observations reflect conditions generally unfavorable for deep moist convection, but several soundings had PW exceeding 50 mm and MLCAPE exceeding 3000 J kg⁻¹. The 0-6-km bulk wind difference was routinely 15-25 m s⁻¹, with some soundings having >40 m s⁻¹; these shear magnitudes supported highly organized convective structures (e.g., Markowski and Richardson 2010; Trapp 2013). However, some mobile soundings during the campaign demonstrated near-storm convective environments comparable to those documented in the more densely observed central US. This large collection of soundings will enable in-depth investigation of the convective environments characteristic of Argentina and facilitate novel comparisons with other regions of the world.

(c) Radars

The CSWR deployed three mobile X-band Doppler on Wheels (DOW) radars (Wurman et al. 1997; 2021) to facilitate targeted observations of the pre-convective environment, storm structures, and boundary layer structures such as gust fronts and other mesoscale boundaries. DOW6 and DOW7 are dual-polarization, dual-frequency Doppler radars. DOW8 was configured as a high power single polarization system for enhanced clear-air sensitivity.

The three DOWs often were deployed to obtain dual- or, in some instances, multi-Doppler coverage of phenomena. Extensive and multiple in-country site surveys were conducted prior to the start of the campaign to identify suitable sites for deployments. The RELAMPAGO sounding, radar, and Pod deployment locations for all missions are shown in Fig. 6.

To facilitate broader coverage over the Córdoba domain by longer-wavelength radars,

CSWR and CSU each provided, deployed, and operated C-band radars. The CSU C-band

radar was operated near Lozada, Córdoba for the period 10 November 2018 – 31 January

2019. The CSU C-band radar was operated in mixed surveillance and Range Height Indicator (RHI) mode; during IOPs the scan strategy was manually adjusted depending on IOP objectives. The CSU C-band documented several tall convective structures (Fig. 7a), including 10 days with 18 dBZ echo tops >16 km MSL, and a storm observed on 25 January 2019 that contained echo tops near 20 km MSL. An example from the tallest storm observed by the CSU C-Band is shown in Figs. 7b-e, with differential reflectivity and specific differential phase columns (e.g., Kumjian et al. 2014), strong C-Band attenuation and differential attenuation (e.g., Rauber and Nesbitt 2018), and a >10-km wide slabular updraft structure apparent in Doppler velocity.

frequency system, and was completed approximately a week before it was shipped to

Argentina for RELAMPAGO. CSWR deployed the radar to near Monte Ralo, Córdoba from

11 November – 14 December 2018. The COW is deployable, with a ~few hour set-up/teardown time, however for logistical reasons the COW remained in the same location for the
duration of the project. Surveillance scan strategies varied depending on the IOP objective. In
total, the CSWR radars collected 351 hours of data during RELAMPAGO.

(d) Deployable hail pads

Penn State University (PSU) deployed hail pads during selected RELAMPAGO IOPs. The hail pads were similar to those used by the CoCoRaHS efforts in the U.S. (Cifelli et al., 2005), deployed in the path of an approaching storm. The hail pads were retrieved and analyzed after storm passage and collected observations during IOP4, IOP9, IOP10, IOP14, and IOP17, and often featured large numbers of impacts by small (<1 cm) hailstones. The PSU team also made post-storm surveys, taking manual measurements of hail sizes with digital calipers. Drone aerial photogrammetry was used during the IOP10, in which size

estimates for nearly 1.6×10^4 hailstones were obtained (Soderholm et al. 2020). These compared favorably to the manual measurements and featured some hail up to 4 cm in maximum dimension. These data will be used for validation of numerical modeling of hail sizes (e.g., Kumjian and Lombardo 2020), and the multi-frequency DOW radar data that have shown promise for use in sizing hail (Kumjian et al. 2018).

(e) Lightning

352

353

354

355

356

357

358

359

360

361

362

363

364

365

366

367

368

369

370

371

372

373

374

375

RELAMPAGO lightning instrumentation, deployed to document the extreme lightning flash rates and storm electrification processes in thunderstorms in SESA (Fig. 8, Table 2) included 10 electric field change meters - the Córdoba Argentina Marx Meter Array (CAMMA, Zhu et al. 2020) deployed by the University of Alabama Huntsville, an 11-station Lightning Mapping Array (LMA) deployed by Marshall Space Flight Center (Lang et al. 2020), 8 electric field mills (EFMs, Antunes de Sa et al. 2020) and four VLF/LF magnetic field receivers – termed Low Frequency Autonomous Magnetic field Sensors (LFAMS), both deployed by the University of Colorado. The Universidad Nacional de Córdoba (UNC) deployed a particle charge sensor. Brazilian National Institute for Space Research installed 3 Transient Luminous Events (TLE) deploy 2 video cameras with low-light level 30 frames/second (fps), and one High Energy Emissions from Thunderstorms station (HEET), with one Neutron Detector, extending the Transient Luminous Event and ThunderstOrm High Energy EmissioN CollAborative Network – LEONA Network (São Sabbas et al. 2017). The LFAMS network extended the lightning detection coverage over the Mendoza region. The LEONA-HEET station was installed at UNC, to detect possible neutron background enhancements and bursts. In order to have an unobstructed view towards the upper atmosphere/near-Earth space region above the RELAMPAGO storms, the 3 LEONA TLE stations were installed ~250-400 km from Córdoba.

376 (f) NCAR WV-DIAL

A Water Vapor Differential Absorption Lidar (WV-DIAL; Spuler et al. 2015; Weckwerth et al. 2016), a compact, field-deployable, micro-pulse differential absorption lidar was deployed at Pilar, Córdoba during IOP. The Water Vapor DIAL provides continuous monitoring of water vapor in the lower troposphere at 150 m range resolution and 1-5 min temporal resolution from 300 m to 4 km AGL in daytime operation with greater range at night. The instrument provided continuous monitoring of lower-tropospheric humidity, cloud base height, and aerosol information east of the SDC.

(g) GOES-16

NOAA's Geostationary Operational Environmental Satellite (GOES-East) located at 75.2W collected 1010 hours of 1-min rapid-scan Mesoscale Domain Sector (MDS) imagery during the period 1 November 2018 - 21 April 2019 in support of RELAMPAGO. For most of the RELAMPAGO missions, the Advanced Baseline Imager (ABI) collected imagery at the 1-min cadence for all 16 spectral bands in the visible (at 500-m resolution) through infrared (at 2-km resolution) wavelengths (Schmit et al. 2017; 2018; Goodman et al. 2019). This was the largest volume of research data collected to date since the launch of the satellite in November 2016. The MDS center point for its 1000 km x 1000 km regional coverage was requested based upon the prior day forecast for possible severe convection within the experiment domain. Concurrent with the 1-min multispectral imagery, the GOES-East Geostationary Lightning Mapper (GLM) collected continuous total lightning (in-cloud and cloud-to-ground) event, stroke, and flash data throughout the day and night with 2-ms temporal resolution and 8-km spatial resolution (Rudlosky et al. 2018). The rapid evolution of GOES-identified overshooting tops, radar, and spaceborne and ground-based lightning structure in a severe hailstorm during RELAMPAGO is examined in Borque et al. (2020).

(h) Brazilian RELAMPAGO component

An observation site near São Borja in far western Rio Grande do Sul state (RS), near the Argentine border (instrumentation listed in Table 3) was coordinated by the Instituto Nacional de Pesquisas Espaciais (INPE) and the Universidade de São Paulo (USP), with the collaboration of the Universidade Federal de Santa Maria (UFSM). The main goals of the this site was to observe mature or decaying stages of convective systems that initiated in north-central Argentina, to observe locally-initiated storms.

During RELAMPAGO at São Borja, five intense convective episodes were observed (Table 5). For most of these cases, data from a single-polarization S-band radar, X-band dual-polarization radar RHIs with high temporal resolution, GOES-16 rapid scans, and successive launches of radiosondes were collected, in addition to the data collected from the network of surface instruments.

(j) Interactions with CACTI

The DOE ARM-funded CACTI field campaign (see companion article by Varble et al. 2021) was planned and operated in coordination with RELAMPAGO to maximize the benefits of each campaign. The CACTI primary observing site near Villa Yacanto in the SDC 20 km east of the mountain ridgeline and the secondary sounding site near Villa Dolores on the plains immediately west of the SDC were frequently used as part of the RELAMPAGO radar, sounding, and surface meteorology networks. The Gulfstream-1 (G-1) aircraft also performed 22 flights during RELAMPAGO. Flight plans and operations depended on forecasting support and real-time flight guidance provided by RELAMPAGO investigators, SMN staff, and graduate students. Nine flights overlapped with RELAMPAGO mobile missions, in which sounding launches and aircraft flight legs were carefully coordinated.

3. RELAMPAGO IOPs

A list of the IOPs during the RELAMPAGO are listed in Table 5. More information and browse imagery are available at the NCAR EOL Field Catalog: http://catalog.eol.ucar.edu/relampago. Each mission was designed to address lighting and hydrometeorology objectives in addition to its primary objectives, and sometimes handoffs (i.e., changes in sampling strategies) from one objective to another occurred during missions.

(a) Convection Initiation

CI IOPs emphasized observation of the mesoscale environments surrounding forecasted regions of deep convection leading up to the initial onset of radar precipitation echoes, making heavy use of the radiosonde resources available for the project to sample the evolution and heterogeneity of CAPE, CIN, and LFC relative to local topographic features, and the radars to identify early stage convective cell locations. There were 7 IOPs dedicated to characterizing environments associated with CI. Five of these were focused near fixed assets in the SDC near Villa Yacanto to maximize observing of forecasted topographic initiation. One mission occurred on the plains east of the SDC, and another occurred in Mendoza province along the Andes foothills. A variety of convective outcomes were observed during CI-focused IOPs: i) 3 days with CI and sustained growth and intensification, ii) 4 days with CI of short-lived, relatively weak precipitation, and iii) 2 days in which little-to-no precipitation was detected at the ground despite forecasts from model forecasts of significant precipitation following CI.

Deployment of RELAMPAGO instrumentation during a typical CI IOP is shown in Fig. 9a. Instruments were deployed several hours prior to the forecasted CI time. Mobile radiosondes were deployed at locations spaced approximately 15-40-km apart, as permitted by the local road network, performing synchronized launches, typically at an hourly frequency.

The hourly launches permit a detailed view of the evolution of stability and moisture surrounding the convective events, including deepening of the boundary layer, detection of probable layers of ascent/descent via tracking of lapse rate and mixing ratio tendency, and erosion of CIN associated with the capping inversion (Fig. 9b). Nelson et al. (2021) analyze considerable spatiotemporal mesoscale heterogeneity among neighboring soundings collected by the radiosonde array during the CI missions, and characterize the statistically significant differences between near-cloud environments supporting or suppressing CI among a sample of 44 radiosondes. Mobile radars were deployed to measure the onset and evolution of precipitation in high resolution during CI, but also targeted clear-air, low-level convergence features (e.g., air mass boundaries and orographic circulations) via dual-Doppler wind retrievals within the boundary layer surrounding CI events (Fig. 9a), revealing the role of initial updraft width in distinguishing successful CI events (Marquis et al. 2021).

(b) Severe convective storms

Severe IOPs were focused on collection of environmental, in-situ, and radar-based storm-scale data to address hypotheses on convective-storm intensity and hazard generation. Because many of the severe-weather hypotheses had linkages to CI and upscale growth, attempts were made for coordinated data collection and mission transfers. IOP selection was prioritized for days on which the meteorological conditions appeared favorable for supercell thunderstorm formation. Three specific mission objectives, namely, (1) the sampling of updrafts, downdrafts, and cold pools to investigate convective-storm dynamics, (2) sampling of hail-growth region to investigate storm microphysics and kinematics, and (3) sampling of severe-wind generation to investigate wind hazards (including tornadic and non-tornadic severe winds), required similar observing strategies. Trapp et al. (2020) details the supercell observed during the 10 November 2018 IOP4. Fig. 10 shows the IOP4 deployment, the GOES-

16 visible image, low-level winds, mid-level updrafts from a DOW multi-Doppler synthesis and GOES-16 overshooting top, and the hail and damage to the COW radar during this storm.

During RELAMPAGO, five IOPs were dedicated to the severe objectives; one of these took place in the Mendoza domain and the remaining four were within the Córdoba domain. In contrast to the supercell occurrence near the SDC during 2015 and 2016 (Mulholland et al. 2018), such occurrence was infrequent during 2018, with supercells observed in only 2 Córdoba IOPs, regardless of the mission objective (Trapp et al. 2020). Of the supercells observed, rotation primarily was confined to the mid- and upper- levels, with low-level rotation observed only in IOP4, aided by the presence of a pre-existing boundary (Kosiba et al. 2020). Hail occurred in 5 IOPs, and was typically <1 cm in maximum dimension (but was as large as 4.3 cm). The two storms observed during the two IOPs in the Mendoza domain were supercells and produced hail; one from the 26 November 2018 IOP 10 is shown in Fig. 11. A supercell resulting from sufficiently strong environmental instability and low-level shear, tracked over the DOW network and produced a long swath of hail. Quantification of the hail fall using drone video and ground reports are described in Solderholm et al. (2020). No tornadoes or wide-spread severe wind events were observed during any of the IOPs. The 5 severe IOPs, coupled with observations from some of the other IOPs, provide a rich data set to examine numerous relationships regarding boundary-storm interactions, relationships between updraft width and overshooting tops, cold pool properties, and storm mode transitions.

(c) Upscale Growth

470

471

472

473

474

475

476

477

478

479

480

481

482

483

484

485

486

487

488

489

490

491

492

493

The overall objective of the upscale growth-related missions in RELAMPAGO was to observe convective lifecycle from initiation through a period of upscale growth, and determine the environmental and terrain-related processes responsible for the rapid growth of these

systems. This strategy included using the DOWs, C-band radars, disdrometers, and 1-minute GOES observations to document storm structures and organization, as well as the three-dimensional hydrometeor distributions throughout convective system evolution. Soundings, mesonet, PODs, and multiple-Doppler wind syntheses are used to describe observed storm structures including convective drafts, cold pools, and gravity waves relative to the topography, the evolution of the synoptic to mesoscale environments, including the role of the SALLJ, and documented processes relevant to backbuilding.

Upscale growth missions collected observations during a variety of MCSs during 5 IOPs in Córdoba with all mobile resources, and 1 IOP (IOP 9b) that documented over 12 h of MCS evolution with the C-band radar network near the SDC while the mobile teams were deployed in Mendoza province. In addition, several MCSs were observed in January during the extended CSU radar operations, CACTI, and enhanced soundings at Córdoba. Fig. 12 shows the backbuilding portion of a massive convective system that stretched to the Atlantic Coast sampled near the SDC during IOP14 on 13-14 December 2018. Convective cells developed within the multi-Doppler domain as shown by the COW image. Mobile soundings indicated adequate conditional instability and deep shear for organized convective structures, with significant local wind profile variability in the SALLJ near the SDC as indicated by the soundings launched at Córdoba and UI1. Upscale growth continued into the evening as the system propagated slowly north, observed by the CSU and RMA1 radars.

4. Inclusivity, education, and outreach

Beyond the invaluable field experience that RELAMPAGO students and early career scientists experienced during RELAMPAGO, an NSF-funded Advanced Studies Institute called Field Studies of Convection in Argentina (ASI-FSCA; Rasmussen et al. 2021) brought 16 students from US graduate programs to Argentina. An NSF Geosciences Opportunities for

Leadership in Diversity (GOLD) training program in preventing harassment during field campaigns was required of all RELAMPAGO participants (Fischer et al. 2021), and the campaign adopted a Code of Conduct and Harassment policy.

RELAMPAGO was a generational opportunity for South American scientists and students, working together on forecasting, observation, and continuing data analysis (Fig. 13, Sidebar 3). A RELAMPAGO open house was held at the Centro Cívico del Bicentenario in downtown Córdoba on 31 October 2018. Several K-12 events reached more than 2,000 students in 15 schools and 3 community centers Córdoba and Sao Borja. During these activities, RELAMPAGO displayed the DOW radars, surface instrumentation, and launched radiosondes with the participants. These events were also accompanied with science talks about hail and flooding from US, Argentine, and Brazilian researchers.

The @RELAMPAGO2018 Twitter account gained over 5,500 followers, and shared tweets in English and Spanish. The @RelampagoEdu Twitter account promoted citizen participation in Spanish, and gathered 690 trustable and geolocated reports used to determine hail size. The twitter account promoted, together with the Province of Córdoba crowdsourcing project *Cosecheros de Granizo* ("hail harvesters"), the dissemination of ~10,000 hail rulers and hail report instructions in Argentina. RELAMPAGO, through sales of campaign t-shirts, donated 15 weather stations and 20 commercial rain gauges to *proyecto MATTEO*, which promotes weather observation in Argentina at local schools. Also, the crowdsourcing campaign *Cazadores de Crecidas* ("flood chasers") allowed the detection of extreme hydrological events by using mobile phones or digital cameras.

Eight scientific videos were created as part of the NCAR Explorer Series that highlight the science and operations of RELAMPAGO-CACTI, as well as career opportunities within the atmospheric and related sciences. These videos show interviews in both English and

Spanish, and will include Spanish subtitles to reach a Spanish speaking audience. The videos are available at: https://ncar.ucar.edu/what-we-offer/education-outreach/public/ncar-explorer-series-field-campaigns/relampago.

5. Summary

RELAMPAGO, together with CACTI, documented continental convection, its internal processes, and its impacts on society in a geographically unique region defined by its significant and complex topography. The observations reveal the unique character of convective systems across the convective spectrum in Argentina that produce high impact weather including hail, flash flooding, and high lightning flash rates in a global convective hotspot.

Together with CACTI, RELAMPAGO has enabled the observation of processes related to orographic CI success and failure with detailed multi-Doppler radar analyses and dense, frequent radiosonde observations that will be used to robustly examine these processes in multi-scale models. The unique storm environments, the role of orographic flows, and storm-internal processes in producing tall, wide convective updrafts, hail-producing but non-tornadic severe convective storms, high lightning flash rates, and rapid convective mode transitions and upscale growth were documented with detailed and comprehensive observations, allowing connections between storm environment, kinematics, and microphysical processes in intense convection to be revealed. Detailed case study analysis and modeling studies of convective storm lifecycle will continue to elucidate how SESA storms fit into the global intense convective spectrum, as well as help meteorological services in SESA improve societal resilience to extreme weather. RELAMPAGO observations has and will continue to help understand the physical processes in severe storms and their impacts, including heavy precipitation and hydrometeorological processes in Argentina,

aiding the global monitoring and prediction of HIW and land-atmosphere interactions on weather and climate timescales.

ACKNOWLEDGMENTS

We also thank all the participants of the campaign, who worked long hours to collect RELAMPAGO data. We thank the National Science Foundation for major support of RELAMPAGO. The authors would like to acknowledge the following NSF grants: AGS-1628708, 1661799, 1661800, 1661679, 1661785, 1661862, 1661726, 1661707, 1661768, 1661657 1661662, 1661863, 1641167, 1835055, and U.S. DOE Office of Science Biological and Environmental Research as part of the Atmospheric System Research program. Research was supported by projects PICT 2017-0221 and UBACyT 20020170100164BA, international cooperation project CONICET - FAPESP 1278/17, CONICET - NSF 2356/18 and SPRINT 3/2016 – FAPESP 2016/50458-1. Thanks also to SPU Res 2018-29 and INVAP S.E. for their contributions.

Major funding for the RELAMPAGO LMA came from the NOAA GOES-R Program,

with additional support from the NASA Lightning Imaging Sensor (LIS) project. NASA GPM-GV also supported the deployment of distrometers. We are grateful to SMN for unconditionally supporting RELAMPAGO operations, forecasting activities, importation/exportation processes, CSWR equipment storage. We also thank all the participants of the campaign, who worked long hours to collect RELAMPAGO data.

The authors would like to acknowledge the following NSF grants: AGS-1628708, 1661799, 1661800, 1661679, 1661785, 1661862, 1661726, 1661707, 1661768, 1661657 1661662, 1661863, 1641167, 1835055, and U.S. DOE Office of Science Biological and

Environmental Research as part of the Atmospheric System Research program. Research was

supported by projects PICT 2017-0221 and UBACyT 20020170100164BA, international

590	cooperation project CONICET - FAPESP 1278/17, CONICET - NSF 2356/18 and SPRINT
591	3/2016 - FAPESP 2016/50458-1. Thanks also to SPU Res 2018-29 and INVAP S.E. for their
592	contributions.
593	RELAMPAGO cannot be possible without the central role of University of Córdoba
594	providing import/export support. The Córdoba provincial government provided the CSU C-
595	Band site, power, and security, organization of open houses, dissemination of RELAMPAGO
596	information, security on roads during mobile operation through multiple agencies: Ministerio
597	de Servicio Públicos; Ministerio de Ciencia y Tecnología; Ministerio de Gobierno. We are
598	also grateful to the national government of Argentina (Ministerio de Ciencia, Tecnología e
599	Innovación, Ministerio de Educación, Ministerio de Relaciones Exteriores, Comercio
600	Internacional y Culto), the US Embassy in Argentina, Empresa Argentina de Navegación
601	Aérea and Centro de la Región Semiárida del Instituto Nacional del Agua. We appreciate
602	INVAP S.E. providing import/export support for CSWR equipment, RMA1 data quality and
603	radar time series storage. RMA1 data was provided by Secretaría de Infraestructura y Política
604	Hídrica, Subsecretaria de Obras Hidráulicas, Ministerio de Obras Públicas. Radar information
605	from San Martín and San Rafael as well as surface data in Mendoza was provided Dirección
606	de Agricultura y Contingencias Climáticas, Mendoza provincial government.
607	Data Availability Statement
608	All RELAMPAGO data are cataloged at the NCAR EOL RELAMPAGO data archive:
609	https://data.eol.ucar.edu/project/RELAMPAGO.
610	Sidebar 1
611	RELAMPAGO Forecast Operations

Forecasting the initiation, location, convective mode, timing, and propagation of deep
convection was critical to the success of RELAMPAGO. A team of forecasters from SMN
and graduate students from US and Argentina universities were assembled to support science
team decisions regarding mobile asset deployment. Forecast briefings were given twice a day
at 1200 and 2100 UTC at the operations center, with an additional 1830 UTC briefing
providing guidance specifically tailored for G-1 operations. On any given day, there were
three forecasters on duty including two SMN personnel providing local knowledge and
expertise. An individual forecaster was available during each mission to monitor current
weather and provide nowcasting guidance. Numerical model guidance was critical to assess
location and intensity of potential deep convection. To this end, University of Illinois (UI),
CSU, Universidad de Buenos Aires (UBA), and SMN provided convection-permitting
regional and global variable resolution runs over the RELAMPAGO region to supplement
global numerical guidance. SMN and Centro de Investigaciones del Mar y la Atmósfera
(UBA) implemented a mesoscale ensemble-based data assimilation and forecast system on
NCAR's Cheyenne supercomputer, which fostered the operational implementation of this
system at SMN.
Since briefings used for operational decision making, the forecasters had to work rapidly
and depend on each other to evaluate and effectively communicate the current weather
situation to the team. Forecasting successful CI was particularly difficult as the convection-
permitting models often produced false alarms. In addition, predictability of severe and
upscale growth events more than 36 hours in advance was sometimes poor, which affected
some deployments, and even a missed upscale growth event in Córdoba while the mobile
teams were in Mendoza (IOP9b). Fortunately, the experimental design and cooperation with

CACTI allowed for observations in the two regions simultaneously. The forecasting team

was truly a cultural exchange experience. The stressful work allowed people of diverse backgrounds to work closely together for several days, creating a truly integrated team. Group photos of the forecast teams are shown in Fig. S1.

639 SIDEBAR 2

Mobile Operations in RELAMPAGO

CSWR provided 3 DOW radars, the COW, 3 mesonets, 12 pods, and 5 sounding systems for the RELAMPAGO project. Three further sounding systems were fielded by universities, two by UI and one by CSU. In total, mobile vehicles drove ~50,000 km throughout the duration of the project. CSWR had an additional 17 participants from multiple outside institutions, including ASI students, constituting a diverse multicultural group (Figure S2). These participants were core to CSWR operations, having mission-critical roles in the preparation and deployment of assets. Each vehicle, and the operations center, had a Spanish-speaking participant to help with logistics and informal outreach during IOPs..

After the daily weather briefing (~12 - 15 hours before departure time), the mission scientist would communicate with the mobile operations coordinator (MOC) and provide a preliminary Google Earth diagram of asset deployment locations. The MOC would refine the deployment locations and distribute the mission asset summary and instrument specific locations to each mobile team. One to two hours prior to departure, the MOC would hold a briefing for the mobile teams and ensure instruments and teams were ready for the mission. After the teams left, the MOC moved to the operations center to provide an interface between mobile assets and the mission scientist, allowing the mission scientist to focus primarily on the evolving event in real time and not the specific deployment and/or instrument details. Communication with the mobile teams was primarily done through WhatsApp, and there

were multiple WhatsApp channels focusing on general and specific mission issues. The MOC monitored and set reasonable crew duty days that satisfied the mission objectives.

SIDEBAR 3

659

660

662

663

664

665

666

667

668

669

670

671

672

673

674

675

676

677

678

679

680

681

682

RELAMPAGO's legacy in Argentina and Brazil: from education to infrastructure

Severe weather researchers and field campaigns concentrated on deep convection in South America can be counted on the fingers of one hand. The remarkable synergy among participants in RELAMPAGO planted the seed of a new generation of scientists in SESA interested in the understanding of deep moist convection through observations and models. Active interactions during and after the campaign keeps this collaboration strong. RELAMPAGO was the first time that SMN engaged in an international field campaign, which is a milestone in scientific and educational cooperation between the SMN, universities and funding agencies in Argentina to support observations. A large group of SMN forecasters had the opportunity to improve their knowledge on nowcasting tools that has improved the weather warning system at SMN. SMN forecasters interacted during RELAMPAGO participants outside of classical forecast operations for the first time. The use of advanced modeling techniques such as model ensembles, data assimilation and rapid refresh models, as well as the collaborative development process undertaken for RELAMPAGO, has and will enable new operational forecast tools and techniques in Argentina. In addition to training in the use of state-of-the-art nowcasting and forecasting tools, participants from different backgrounds (e.g., hydrologists, engineers, and others) took advantage of the forecast briefings at the Operational Center to understand HIW forecasting and learned how weather forecast tools could be applied to infrastructure. This motivated the implementation of real-time forecasts for water resources management and hydrologic risk mitigation in the flash flood-prone river basins in the SDC.

683	REFERENCES
684	Altinger de Schwarzkopf, M. L., and L. C. Rosso, 1982: Severe Storms and Tornadoes in
685	Argentina. 12th Conference on Severe Local Storms, American Meteorological
686	Society, 59-62.
687	Alvarez Imaz, M., P. Salio, M. Dillon, L. Fita Borell, 2020: The role of atmospheric forcings
688	and WRF physical set-up on convective initiation over Córdoba, Argentina.
689	Atmospheric Research, in Review.
690	Anabor, V., D. J. Stensrud, and O. L. L. de Moraes, 2008: Serial Upstream-Propagating
691	Mesoscale Convective System Events over Southeastern South America. Mon. Wea.
692	Rev., 136, 3087–3105, https://doi.org/10.1175/2007MWR2334.1
693	Anabor, V., D. J. Stensrud, and O. L. L. de Moraes, 2009: Simulation of a Serial Upstream-
694	Propagating Mesoscale Convective System Event over Southeastern South America
695	Using Composite Initial Conditions. Mon. Wea. Rev., 137, 2144–2163,
696	https://doi.org/10.1175/2008MWR2617.1
697	Antunes de Sa, A.,R.A. Marshall, A.P. Sousa and W. Deierling, 2020: An array of low-cost,
698	high-speed autonomous electric field mills for thunderstorm research. Earth and
699	Space Science. Conditionally accepted.
700	Bang, S. D., and D. J. Cecil, 2019: Constructing a Multifrequency Passive Microwave Hail
701	Retrieval and Climatology in the GPM Domain. J. Appl. Meteor. Climatol., 58, 1889-
702	1904, https://doi.org/10.1175/JAMC-D-19-0042.1
703	Banta, R. M., and C. Barker Schaaf, 1987: Thunderstorm Genesis Zones in the Colorado
704	Rocky Mountains as Determined by Traceback of Geosynchronous Satellite Images.

705	Mon. Wea. Rev., 115, 463–476, https://doi.org/10.1175/1520-
706	0493(1987)115<0463:TGZITC>2.0.CO;2
707	Barnes G., 2001: Severe Local Storms in the Tropics. In: Doswell C.A. (eds) Severe
708	Convective Storms. Meteorological Monographs. American Meteorological Society,
709	Boston, MA. https://doi.org/10.1007/978-1-935704-06-5_10
710	Battaglia, A., E. Rustemeier, A. Tokay, U. Blahak, and C. Simmer, 2010: PARSIVEL Snow
711	Observations: A Critical Assessment. J. Atmos. Oceanic Technol., 27, 333-344,
712	https://doi.org/10.1175/2009JTECHA1332.1
713	Borque, P., P. Salio, M. Nicolini, and Y. García Skabar, 2010: Environment Associated with
714	Deep Moist Convection under SALLJ Conditions: A Case Study. Wea. Forecasting,
715	25, 970–984, https://doi.org/10.1175/2010WAF2222352.1
716	Borque, P., Vidal, L., Rugna, M., Lang, T. J., Nicora, M. G., and Nesbitt, S.
717	W. (2020). Distinctive signals in 1- min observations of overshooting tops and
718	lightning activity in a severe supercell thunderstorm. J. Geophys. Res.: Atmos., 125,
719	e2020JD032856. https://doi.org/10.1029/2020JD032856
720	Brooks, H. and C. A. Doswell,2001: Some aspects of the international climatology of
721	tornadoes by damage classification, Atmospheric Research, 56, 1-4, 191-
722	201,https://doi.org/10.1016/S0169-8095(00)00098-3
723	Brooks, H. E., and Correia, J., Jr., 2018: Long-Term Performance Metrics for National
724	Weather Service Tornado Warnings. Wea. Forecast., 33, 6, 1501-1511,
725	https://doi.org/10.1175/WAF-D-18-0120.1
726	Cancelada, M.; Salio, P.; Vila, D.; Nesbitt, S.W.; Vidal, L. Backward Adaptive Brightness
727	Temperature Threshold Technique (BAB3T): A Methodology to Determine Extreme

728	Convective Initiation Regions Using Satellite Infrared Imagery. Remote Sens. 2020,
729	12, 337; https://doi.org/10.3390/rs12020337
730	Carbone, R. E., J. D. Tuttle, D. A. Ahijevych, and S. B. Trier, 2002: Inferences of
731	Predictability Associated with Warm Season Precipitation Episodes. J. Atmos. Sci.,
732	59, 2033–2056, https://doi.org/10.1175/1520-
733	0469(2002)059<2033:IOPAWW>2.0.CO;2
734	Carril, A.F., Menéndez, C.G., Remedio, A.R.C. et al. Performance of a multi-RCM ensemble
735	for South Eastern South America. Clim Dyn 39, 2747–2768 (2012).
736	https://doi.org/10.1007/s00382-012-1573-z
737	Cecil, D. J., S. J. Goodman, D. J. Boccippio, E. J. Zipser, and S. W. Nesbitt, 2005: Three
738	Years of TRMM Precipitation Features. Part I: Radar, Radiometric, and Lightning
739	Characteristics. Mon. Wea. Rev., 133, 543–566, https://doi.org/10.1175/MWR-2876.1
740	Cecil, D. J., and C. B. Blankenship, 2012: Toward a Global Climatology of Severe
741	Hailstorms as Estimated by Satellite Passive Microwave Imagers. J. Climate, 25, 687-
742	703, https://doi.org/10.1175/JCLI-D-11-00130.1
743	Cifelli, R., N. Doesken, P. Kennedy, L. D. Carey, S. A. Rutledge, C. Gimmestad, and T.
744	Depue, 2005: The Community Collaborative Rain, Hail, and Snow Network: Informal
745	Education for Scientists and Citizens. Bull. Amer. Meteor. Soc., 86, 1069-1078,
746	https://doi.org/10.1175/BAMS-86-8-1069
747	Davis, C., N. Atkins, D. Bartels, L. Bosart, M. Coniglio, G. Bryan, W. Cotton, D. Dowell, B.
748	Jewett, R. Johns, D. Jorgensen, J. Knievel, K. Knupp, WC. Lee, G. McFarquahar, J.
749	Moorse, R. Przybylinski, R. Rabuer, B. Smull, R. Trapp, S. Trier, R. Wakimoto, M.

750	Weisman, and C. Ziegler, 2004: The Bow Echo and MCV Experiment: Observations
751	and Opportunities. Bulletin of the American Meteorological Society, 85, 1075-1092.
752	Del Genio, A. D., J. Wu, and Y. Chen, 2012: Characteristics of Mesoscale Organization in
753	WRF Simulations of Convection during TWP-ICE. J. Climate, 25, 5666-5688,
754	https://doi.org/10.1175/JCLI-D-11-00422.1
755	Doswell, C. A., H. E. Brooks, and R. A. Maddox, 1996: Flash Flood Forecasting: An
756	Ingredients-Based Methodology. Wea. Forecasting, 11, 560-581,
757	https://doi.org/10.1175/1520-0434(1996)011<0560:FFFAIB>2.0.CO;2
758	Durkee, J. D., T. L. Mote, and J. M. Shepherd, 2009: The Contribution of Mesoscale
759	Convective Complexes to Rainfall across Subtropical South America. J. Climate, 22,
760	4590–4605, https://doi.org/10.1175/2009JCLI2858.1
761	Falco, M., Carril, A.F., Menéndez, C.G. et al. Assessment of CORDEX simulations over
762	South America: added value on seasonal climatology and resolution considerations.
763	Clim Dyn 52, 4771–4786 (2019). https://doi.org/10.1007/s00382-018-4412-z
764	Fischer, E. V., B. Bloodhart, K. Rasmussen, I. B. Pollack, M. G. Hastings, E. Marin-Spiotta,
765	A. R. Desai, J. P. Schwarz, S. Nesbitt and D. Hence, 2020: Leveraging Field-
766	Campaign Networks to Effect Collaborative Change on Sexual Harassment. Bull.
767	Amer. Meteor. Soc., in Review.
768	Geerts, B., Parsons, D., Ziegler, C. L., Weckwerth, T. M., Biggerstaff, M. I., Clark, R. D.,
769	Coniglio, M. C., Demoz, B. B., Ferrare, R. A., Gallus, W. A., Jr., Haghi, K.,
770	Hanesiak, J. M., Klein, P. M., Knupp, K. R., Kosiba, K., McFarquhar, G. M., Moore,
771	J. A., Nehrir, A. R., Parker, M. D., Pinto, J. O., Rauber, R. M., Schumacher, R. S.,
772	Turner, D. D., Wang, Q., Wang, X., Wang, Z., and Wurman, J. (2017). The 2015

113	Plains Elevated Convection at Night Field Project. Bulletin of the American
774	Meteorological Society 98, 4, 767-786, https://doi.org/10.1175/BAMS-D-15-00257.1
775	Goodman, S. J., T. J. Schmit, J. Daniels, and R. J. Redmon, eds., 2019: The GOES-R Series:
776	A New Generation of Geostationary Environmental Satellites, Academic Press, Print
777	and e-book, ISBN-13: 978-0128143278, ISBN-10: 0128143274, 306 pp.
778	Heim, C., D. Panosetti, L. Schlemmer, D. Leuenberger, and C. Schär, 2020: The Influence of
779	the Resolution of Orography on the Simulation of Orographic Moist Convection.
780	Mon. Wea. Rev., 148, 2391–2410, https://doi.org/10.1175/MWR-D-19-0247.1
781	Herman, G. R., Nielsen, E. R., and Schumacher, R. S., 2018: Probabilistic Verification of
782	Storm Prediction Center Convective Outlooks. Wea. Forecast, 33, 1, 161-184,
783	https://doi.org/10.1175/WAF-D-17-0104.1
784	Houze, R. A., Rasmussen, K. L., Zuluaga, M. D., and Brodzik, S. R.,,2015: The variable
785	nature of convection in the tropics and subtropics: A legacy of 16 years of the
786	Tropical Rainfall Measuring Mission satellite, Rev. Geophys., 53, 994–1021,
787	doi:10.1002/2015RG000488
788	Kirshbaum, D. J., 2013: On Thermally Forced Circulations over Heated Terrain. J. Atmos.
789	Sci., 70, 1690–1709, https://doi.org/10.1175/JAS-D-12-0199.1
790	Kirshbaum, D. J., and C. Wang, 2014: Boundary Layer Updrafts Driven by Airflow over
791	Heated Terrain. J. Atmos. Sci., 71, 1425-1442, https://doi.org/10.1175/JAS-D-13-
792	0287.1
793	Kumjian, M. R., A. P. Khain, N. Benmoshe, E. Ilotoviz, A. V. Ryzhkov, and V. T. J. Phillips
794	2014: The Anatomy and Physics of Z_{DR} Columns: Investigating a Polarimetric Radar

795	Signature with a Spectral Bin Microphysical Model. J. Appl. Meteor. Climatol., 53,
796	1820–1843, https://doi.org/10.1175/JAMC-D-13-0354.1.
797	Kumjian, M. R., Y. P. Richardson, T. Meyer, K. A. Kosiba, and J. Wurman, 2018: Resonance
798	Scattering Effects in Wet Hail Observed with a Dual-X-Band-Frequency, Dual-
799	Polarization Doppler on Wheels Radar. J. Appl. Meteor. Climatol., 57, 2713–2731,
800	https://doi.org/10.1175/JAMC-D-17-0362.1
801	Kumjian, M. R., and Coauthors, 2020: Gargantuan Hail in Argentina. Bull. Amer. Meteor.
802	Soc., 101, E1241–E1258, https://doi.org/10.1175/BAMS-D-19-0012.1
803	Kumjian, M. R., and K. Lombardo, 2020: A hail growth trajectory model for exploring the
804	environmental controls on hail size: Model physics & idealized tests. Journal of the
805	Atmospheric Sciences, 77, 2765–2791, https://doi.org/10.1175/JAS-D-20-0016.1
806	Lang, T. J., and Coauthors, The RELAMPAGO Lightning Mapping Array: Overview and
807	initial comparison to the Geostationary Lightning Mapper. J. Atmos. Oceanic
808	Technol., doi: https://doi.org/10.1175/JTECH-D-20-0005.1
809	Marengo, J. A., W. R. Soares, C. Saulo, and M. Nicolini, 2004: Climatology of the Low-
810	Level Jet East of the Andes as Derived from the NCEP-NCAR Reanalyses:
811	Characteristics and Temporal Variability. J. Climate, 17, 2261-2280,
812	https://doi.org/10.1175/1520-0442(2004)017<2261:COTLJE>2.0.CO;2
813	Markowski P. and Y. Richardson 2010: Mesoscale Meteorology in Mid-Latitudes
814	https://doi.org/10.1002/9780470682104
815	Marquis, J. N., A. Varble, P. Robinson, T. C. Nelson, and K. Friederich, 2021: Low-level
816	Mesoscale and Cloud-scale Interactions Promoting Deep Convection Initiation. Mon.
817	Wea. Rev., in review.

818	Martinez, J. A., and F. Dominguez, 2014: Sources of Atmospheric Moisture for the La Plata
819	River Basin. J. Climate, 27, 6737–6753, https://doi.org/10.1175/JCLI-D-14-00022.1
820	Matsudo, C.M. and Salio, P. 2011: Severe weather reports and proximity to deep convection
821	over Northern Argentina. Atmospheric Research, 100, 4, 523-537,
822	http://dx.doi.org/10.1016/j.atmosres.2010.11.004
823	Mezher R., M. Doyle and V. Barros, 2012: Climatology of hail in Argentina, Atmospheric
824	Research, 114–115, 70-82, https://doi.org/10.1016/j.atmosres.2012.05.020
825	Mulholland, J. P., S. W. Nesbitt, R. J. Trapp, K. L. Rasmussen, and P. V. Salio, 2018:
826	Convective Storm Life Cycle and Environments near the Sierras de Córdoba,
827	Argentina. Mon. Wea. Rev., 146, 2541–2557, https://doi.org/10.1175/MWR-D-18-
828	0081.1
829	Nelson, T.C., J. Marquis, A. Varble, K. Friedrich, 2021: Radiosonde Observations of
830	Environments Supporting Deep Moist Convection Initiation During RELAMPAGO-
831	CACTI. Mon. Wea. Rev., accepted.
832	National Academies of Sciences, Engineering, and Medicine. 2016. Attribution of Extreme
833	Weather Events in the Context of Climate Change. Washington, DC: The National
834	Academies Press. https://doi.org/10.17226/21852.
835	Nesbitt, S. W., R. Cifelli, and S. A. Rutledge, 2006: Storm Morphology and Rainfall
836	Characteristics of TRMM Precipitation Features. Mon. Wea. Rev., 134, 2702–2721,
837	https://doi.org/10.1175/MWR3200.1
838	Nicolini, M., C. Saulo, J. C. Torres, and P. Salio, 2002: Strong South American low-level jet
839	events characterization during warm season and implications for enhanced

840	precipitation, Meteorologica (Special Issue on South American Moonsoon System)
841	27, 59-69.
842	Nicolini, M. and A.C. Saulo, 2006: Modeled Chaco low-level jets and related precipitation
843	patterns during the 1997–1998 warm season. Meteorol. Atmos. Phys. 94, 129–143.
844	https://doi.org/10.1007/s00703-006-0186-7
845	Nicolini M and Y. García Skabar, 2011: Diurnal cycle in convergence patterns in the
846	boundary layer east of the Andes and convection, Atmospheric Research, 100, 4, 377-
847	390, https://doi.org/10.1016/j.atmosres.2010.09.019
848	Panosetti, D., L. Schlemmer and C. Schär, 2020. Convergence behavior of idealized
849	convection-resolving simulations of summertime deep moist convection over land.
850	Clim Dyn 55, 215–234. https://doi.org/10.1007/s00382-018-4229-9
851	Peters, J. M., and R. S. Schumacher, 2015: The Simulated Structure and Evolution of a
852	Quasi-Idealized Warm-Season Convective System with a Training Convective Line.
853	J. Atmos. Sci., 72, 1987–2010, https://doi.org/10.1175/JAS-D-14-0215.1.
854	Peterson, M. J., Lang, T. J., Bruning, E. C., Albrecht, R., Blakeslee, R. J., Lyons, W. A., et al,
855	2020: New World Meteorological Organization certified megaflash lightning
856	extremes for flash distance (709 km) and duration (16.73 s) recorded from space.
857	Geophysical Research Letters, 47, e2020GL088888.
858	https://doi.org/10.1029/2020GL088888
859	Rauber, R. M., and S. W. Nesbitt, 2018: Radar meteorology, a first course. Wiley. 461pp.
860	Rasmussen, K. L., and Houze, R. A., Jr., 2011: Orogenic Convection in Subtropical South
861	America as Seen by the TRMM Satellite. Mon. Wea. Rev., 139, 8, 2399-2420,
862	https://doi.org/10.1175/MWR-D-10-05006.1

863	Rasmussen, K. L., Zuluaga, M. D., and Houze, R. A., 2014: Severe convection and lightnin
864	in subtropical South America, Geophys. Res. Lett., 41, 7359-7366,
865	doi:10.1002/2014GL061767
866	Rasmussen, K. L., and R. A. Houze, 2016: Convective Initiation near the Andes in
867	Subtropical South America. Mon. Wea. Rev., 144, 2351–2374,
868	https://doi.org/10.1175/MWR-D-15-0058.1.
869	Rasmussen, K. L., M. M. Chaplin, M. D. Zuluaga, and R. A. Houze, 2016: Contribution of
870	Extreme Convective Storms to Rainfall in South America. J. Hydrometeor., 17, 353-
871	367, https://doi.org/10.1175/JHM-D-15-0067.1.
872	Rasmussen, K. L., M. A. Burt, A. Rowe, R. Haacker, D. Hence, L. M. Luna, S. W. Nesbitt,
873	and J. Maertens, 2020: Enlightenment strikes! Broadening graduate school training
874	through field campaign participation. Bull. Amer. Meteor. Soc., submitted.
875	Ribeiro, B. Z., and L. F. Bosart, 2018: Elevated Mixed Layers and Associated Severe
876	Thunderstorm Environments in South and North America. Mon. Wea. Rev., 146, 3-
877	28, https://doi.org/10.1175/MWR-D-17-0121.1.
878	Rudlosky, S. D., S. J. Goodman, K. S. Virts, and E. C. Bruning, 2018: Initial Geostationary
879	Lightning Mapper Observations, Geophys. Res. Lett., DOI:10.1029/2018GL081052.
880	Salio, P., Nicolini, M., and Saulo, A. C., 2002: Chaco low-level jet events characterization
881	during the austral summer season, J. Geophys. Res., 107(D24), 4816,
882	doi:10.1029/2001JD001315.
883	Salio, P., M. Nicolini, and E. J. Zipser, 2007: Mesoscale Convective Systems over
884	Southeastern South America and Their Relationship with the South American Low-
885	Level Jet. Mon. Wea. Rev., 135, 1290–1309, https://doi.org/10.1175/MWR3305.1.

886	São Sabbas Tavares, F., and coauthors, 2017: LEONA for TLE and HEET Research in South
887	America. AGU Fall Meeting, New Orleans, Louisiana.
888	Saulo, A. C., M. E. Seluchi, and M. Nicolini, 2004: A Case Study of a Chaco Low-Level Jet
889	Event. Mon. Wea. Rev., 132, 2669–2683, https://doi.org/10.1175/MWR2815.1.
890	Saulo, A. C., J. Ruiz, and Y. G. Skabar, 2007: Synergism between the Low-Level Jet and
891	Organized Convection at Its Exit Region. Mon. Wea. Rev., 135, 1310-1326,
892	https://doi.org/10.1175/MWR3317.1.
893	Schaaf, C. B., J. Wurman, and R. M. Banta, 1988: Thunderstorm-Producing Terrain Features.
894	Bull. Amer. Meteor. Soc., 69, 272–277, https://doi.org/10.1175/1520-
895	0477(1988)069<0272:TPTF>2.0.CO;2.
896	Schmit, T. J., Paul Griffith, Mathew M. Gunshor, Jaime M. Daniels, Steven J. Goodman and
897	William J. Lebair, 2017: A Closer Look at the ABI on the GOES-R Series, Bull. Am.
898	Meteor. Soc., DOI: 10.1175/BAMS-D-15-00230.1.
899	Schmit, T.J., Lindstrom, S.S., Gerth, J.J., Gunshor, M.M., 2018. Applications of the 16
900	spectral bands on the Advanced Baseline Imager (ABI), J. Oper. Meteor. 6 (4), 33-46.
901	https://doi.org/10.15191/nwajom.2018.0604.
902	Schumacher, R. S., 2015: Sensitivity of Precipitation Accumulation in Elevated Convective
903	Systems to Small Changes in Low-Level Moisture. J. Atmos. Sci., 72, 2507–2524,
904	https://doi.org/10.1175/JAS-D-14-0389.1
905	Schumacher R. and coauthors, 2020: Convective-storm environments in subtropical South
906	America from high-frequency soundings during RELAMPAGO-CACTI. Mon. Wea.
907	Rev., in review.

908	Seluchi, M. E., A. C. Saulo, M. Nicolini, and P. Satyamurty, 2003: The Northwestern
909	Argentinean Low: A Study of Two Typical Events. Mon. Wea. Rev., 131, 2361-
910	2378, https://doi.org/10.1175/1520-0493(2003)131<2361:TNALAS>2.0.CO;2.
911	Shapiro, M. A., 1981: Frontogenesis and Geostrophically Forced Secondary Circulations in
912	the Vicinity of Jet Stream-Frontal Zone Systems. J. Atmos. Sci., 38, 954-973,
913	https://doi.org/10.1175/1520-0469(1981)038<0954:FAGFSC>2.0.CO;2.
914	Soderholm J.S., M.R. Kumjian, N. McCarthy, P. Maldonado, and M. Wang, 2020:
915	Quantifying hail size distributions from the sky – application of drone aerial
916	photogrammetry. Atmos. Meas. Tech., 13, 747–754, https://doi.org/10.5194/amt-13-
917	747-2020, 2020
918	Spuler S., K. Repasky, B. Morley, D. Moen, T. Weckwerth, M. Hayman, and A. Nehrir 2015:
919	Advances in Diode-Laser-Based Lidar for Profiling Atmospheric Water Vapor, OSA
920	Technical Digest. https://doi.org/10.1364/CLEO_AT.2015.ATu4J.7
921	Stanfield, R. E., X. Dong, B. Xi, A. Kennedy, A. D. Del Genio, P. Minnis, and J. H. Jiang,
922	2014: Assessment of NASA GISS CMIP5 and Post-CMIP5 Simulated Clouds and
923	TOA Radiation Budgets Using Satellite Observations. Part I: Cloud Fraction and
924	Properties. J. Climate, 27, 4189–4208, https://doi.org/10.1175/JCLI-D-13-00558.1
925	Thompson, R. L., B. T. Smith, J. S. Grams, A. R. Dean, and C. Broyles, 2012: Convective
926	Modes for Significant Severe Thunderstorms in the Contiguous United States. Part II:
927	Supercell and QLCS Tornado Environments. Wea. Forecasting, 27, 1136–1154,
928	https://doi.org/10.1175/WAF-D-11-00116.1.
929	Trapp R.J, N.S. Diffenbaugh, H.E. Brooks, M.E. Baldwin, E.D. Robinson, J.S. Pal, 2007:
930	Changes in severe thunderstorm environment frequency during the 21st century

931	caused by anthropogenically enhanced global radiative forcing. Proceedings of the
932	National Academy of Sciences, 104 (50) 19719-19723; DOI:
933	10.1073/pnas.0705494104
934	Trapp, R. J., and Coauthors, 2020: Multiple-Platform and Multiple-Doppler Radar
935	Observations of a Supercell Thunderstorm in South America during RELAMPAGO.
936	Mon. Wea. Rev., 148, 3225–3241, https://doi.org/10.1175/MWR-D-20-0125.1
937	Trapp, R.J., 2013: Mesoscale-Convective Processes in the Atmosphere, Cambridge
938	University Press, 346 pp. https://doi.org/10.1017/CBO9781139047241
939	Tucker, D. F., and N. A. Crook, 2005: Flow over Heated Terrain. Part II: Generation of
940	Convective Precipitation. Mon. Wea. Rev., 133, 2565-2582,
941	https://doi.org/10.1175/MWR2965.1
942	van der Ent, R. J., Savenije, H. H. G., Schaefli, B., and Steele- Dunne, S. C., 2010: Origin
943	and fate of atmospheric moisture over continents, Water Resour. Res., 46, W09525,
944	doi:10.1029/2010WR009127
945	Varble A. and Coauthors, 2020: Utilizing a Storm-Generating Hotspot to Study Convective
946	Cloud Transitions: The CACTI Experiment. Bull. Amer. Meteor. Soc., in Review.
947	Velasco, I., and Fritsch, J. M. ,1987: Mesoscale convective complexes in the Americas, J.
948	Geophys. Res., 92(D8), 9591–9613, doi:10.1029/JD092iD08p09591
949	Vera, C., and Coauthors, 2006: The South American Low-Level Jet Experiment. Bull. Amer
950	Meteor. Soc., 87, 63–78, https://doi.org/10.1175/BAMS-87-1-63
951	Vidal, L., 2014: Extreme convection over South America: internal structure, life cycles and
952	influence of topography on initiation. Doctoral Thesis. University of Buenos Aires.

953	Faculty of Exact and Natural Sciences (in Spanish)
954	http://hdl.handle.net/20.500.12110/tesis_n5573_Vidal
955	Weckwerth, T. M., K. J. Weber, D. D. Turner, and S. M. Spuler, 2016: Validation of a Water
956	Vapor Micropulse Differential Absorption Lidar (DIAL). J. Atmos. Oceanic Technol.,
957	33, 2353–2372, https://doi.org/10.1175/JTECH-D-16-0119.1
958	Wilson, J. W., and C. K. Mueller, 1993: Nowcasts of Thunderstorm Initiation and Evolution.
959	Wea. Forecasting, 8, 113–131, https://doi.org/10.1175/1520-
960	0434(1993)008<0113:NOTIAE>2.0.CO;2
961	Wurman, J., J. Straka, E. Rasmussen, M. Randall, and A. Zahrai, 1997: Design and
962	Deployment of a Portable, Pencil-Beam, Pulsed, 3-cm Doppler Radar. J. Atmos.
963	Oceanic Technol., 14, 1502-1512, https://doi.org/10.1175/1520-
964	0426(1997)014<1502:DADOAP>2.0.CO;2
965	Zhong S.and F.K. Chow, 2013: Meso- and Fine-Scale Modeling over Complex Terrain:
966	Parameterizations and Applications. In: Chow F., De Wekker S., Snyder B. (eds)
967	Mountain Weather Research and Forecasting. Springer Atmospheric Sciences.
968	Springer, Dordrecht. https://doi.org/10.1007/978-94-007-4098-3_10
969	Zhu, Y., Bitzer, P., Stewart, M., Podgorny, S., Corredor, D., Burchfield, J., et al. (2020).
970	Huntsville Alabama Marx Meter Array 2: Upgrade and capability. Earth and Space
971	Science, 7, e2020EA001111.https://doi.org/10.1029/2020EA001111
972	Zipser, E. J., C. Liu, D. J. Cecil, S. W. Nesbitt, and D. P. Yorty, 2006: Where are the most
973	intense thunderstorms on Earth? Bull. Amer. Meteor. Soc., 87, 1057-1071,
974	doi:https://doi.org/10.1175/BAMS-87-8-1057

976 TABLES

977 Table 1. RELAMPAGO in a nutshell.

RELAMPAGO in a nutshell

6 years planning the field campaign. 3 site surveys before the campaign. More than 10,000 km toured to determine possible deployment sites.

234 scientists, technicians and students at the Operational Center from 6 countries (USA, Argentina, Brazil, Australia, Spain, and UK)

94 graduate and undergraduate students from USA (51), Argentina (34), Brazil (5), Australia (2), Spain (1) and UK (1) participated in the field campaign

16 universities and research centers collaborating for RELAMPAGO organization and deployment from 3 countries (USA, Argentina and Brazil).

2 forecast dry-runs before the campaign. 89 forecast briefings during the campaign. 3 mesoscale forecast models and 1 60-member model ensemble ran over the RELAMPAGO domain.

5 research themes: Convective initiation, Severe convective weather, Upscale growth of convection, Lightning, and Hydrometeorology.

47 IOP days directed from the operations center at Villa Carlos Paz.

19 Missions: 3 DOWs, 1 COW, 3 mesonets, 12 Pods, 3 disdrometers, 6 sounding operating units driven more than 30,000 km. 3 Operational and 1 fixed sounding station with additional observations per request from the RELAMPAGO team.

1192 fixed and mobile soundings.

3 ground-based C-band radars operating over the RELAMPAGO Córdoba sector.

1010 hours of GOES-16 Mesoscale Domain Sector observations during EOP and IOP.

> 49 million raindrops measured by RELAMPAGO disdrometers.

2285 impacts on RELAMPAGO deployed hailpads. 2 storms reaching more than 18 km in altitude. More than 45,000 GOES over-shooting tops during EOP. 2.9 million lightning flashes observed with a lightning mapping array over 163 days. 3 river basins observed and runoff-rating curves determined. 21 terabytes of mobile radar data collected. 1 Open House at Córdoba, 2 Open houses in collaboration with CACTI, 15 visits at schools and community centers. More than 5,000 people were interacted with. Innumerable people stopped at instrumentation on the roads during RELAMPAGO deployments. 5,500 followers at the @RELAMPAGO2018 Twitter account. 690 severe weather reports received using the @RelampagoEdu Twitter account. 3 citizen crowdsourcing projects, dissemination of ~10K hail rulers. 19 institutions and local government agencies hosting instruments, 25 families hosting instruments at their own homes or farms.

978

979

980

981

982

Instrumentation and Measured quantity	Detection Frequency Regime/ E nergy range	Temporal Resolution	Data Products	Purpose
NASA LMA radio emissions from lightning	60-66 MHz (11 stations)	~1 µs	Sources, Flashes	GLM validation, total lightning activity, areal extent, and propagation
UAH CAMMA VLF/MF electric field change	Slow: 1 Hz - 57 kHz Fast: 1.6 kHz - 2.5 MHz	Slow: ~1 μs Fast: ~100 ns	L0 (L1): raw (QC'ed) waveform L2: sources	Slow: charge retrieval, continuing current, flash energy Fast: lightning mapping, peak current, flash type
CU LFAMS radio emissions from lightning	1-400 kHz	1 μs	Raw QC'ed waveform as well as stroke time, location and peak current	Lightning flash rates and geolocation over larger domain covering also the Mendoza region
INPE LEONA Network (a) Transient Luminous Events (TLEs) (b) atmospheric neutrons	(a) 30 fps low-light level video cameras (b) 16.7 Hz- 1 kHz Thermal (~0,025 eV) neutron detector	(a) ~16.7 ms (b) Fast: 1 ms Slow: 1 min	(a) TLE occurrence, type, duration and location (b) Neutron count, enhancement/ burst occurrence and duration	(a) TLE detection and characterization (b) Thunderstorm/lightning excited neutron emission measurement
CU EFM vertical electric field	DC to 100 Hz	1 ms	Electric field amplitude and polarity	Electric field of storms overhead
UNC particle charge sensor (PCS) Induced charge and raindrop fall velocity			Sign and magnitude of the charge and size of raindrops	

987 Table 3: Instruments at the Brazil Site in São Borja.

Measurement	Sensors
Radars	Gematronik X-Band radar
Surface Meteorology	4 micronet stations measuring temperature, dewpoint
	temperature, atmospheric pressure, and wind speed and
	direction, accumulated rainfall
Precipitation	Parsivel2 disdrometer
	Joss-Waldvogel disdrometer
	Tipping bucket rain gauge
Electrification	4 electric field mills
Total column water vapor	2 GPS systems
Upper air soundings	Launched daily at 1800 UTC and sequentially during
	storm events
Hail	Hail pads

989

Table 4: Storms sampled by the RELAMPAGO-Brazil observational site in Sao Borja, RioGrande do Sul, Brazil.

Type of Event
Intense QLCS with
bowing segment
Large MCS causing local
flash floods
Supercell producing a
downburst
Gust front associated with
a nocturnal QLCS
Intense nocturnal storms

Table 5: RELAMPAGO IOPs. IOPs are classified by their primary objective resulting in 8 Convective Initiation (CI) IOPs, 6 Upscale Growth (UG) IOPs, 5 Severe Weather (SW) IOPs, and 1 Unclassified IOP.

IOP Number	Date	Primary Mission Type	CSWR Radars	Radar Scan Mode	Number of Soundings	Number of Pods	Mesonet Data
1	11/02	CI	DOW 6, 7, 8	CI	10	10	Y
2	11/05	UG	DOW 7, 8	UG	12	7	Y
3	11/06	CI	DOW 7,8	CI	21	9	Y
4	11/10	SW	DOW 6, 7, 8	CI/SW	27	11	Y
5	11/12	UG	DOW 6, 7, 8	UG	40	9	Y
6	11/17	No classification	N/A	N/A	28	0	N
7	11/21	CI	DOW 6, 7, 8, C- band	CI	30	11	Y
8	11/22	SW	DOW 6, 7, 8, C-band	CI/S	23	12	Y
9a	11/25	SW	DOW 6, 7, 8	SW	22	12	Y
9b	11/26	UG	C-band	UG	0	0	N
10	11/26	CI	DOW 7, 8	CI/SW	28	12	Y

11	11/29	CI	DOW, 7, 8 C-band	CI/SW	30	12	Y
12	11/30	UG	DOW, 7, 8 C-band	CI/UG	42	8	Y
13	12/04	CI	DOW 6, 7, 8, C- band	CI/SW	33	12	Y
14	12/05	UG	DOW 6, 7, 8, C- band	CI/UG	35	9	Y
15	12/10	SW	DOW 6, 7, 8	CI	6	9	Y
16	12/11	SW	DOW 6, 7, 8, C- band	CI	14	9	Y
17	12/13	UG	DOW, 7, 8 C-band	CI/UG	27	6	Y
18	12/16	CI	DOW, 7, 8	CI	21	12	Y
19	12/17	CI	DOW7	CI	24	10	Y

998 FIGURES

999

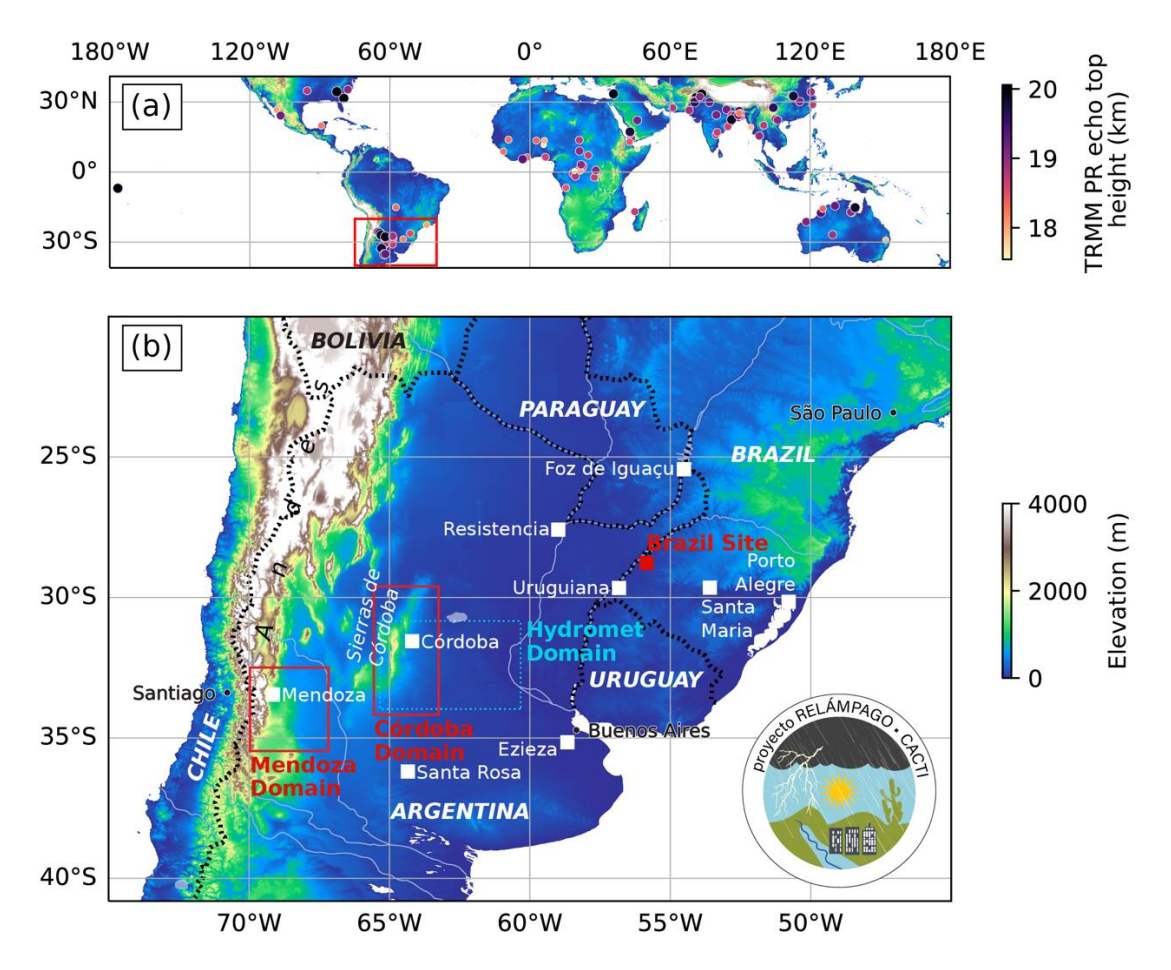


Fig. 1. (a) TRMM precipitation radar (PR) December 1998 – September 2013 observed echo top heights in the 99.9999th percentile (following Zipser et al. 2006). The region in panel (b) is shown by the red box. (b) RELAMPAGO mobile observation domains (red boxes, see Fig. 6), Brazil Site (red square), operational sounding sites (white squares), and hydrometeorology observation domain (cyan dashed box, see Fig. 4). Terrain elevation (m MSL) is shaded in each figure.

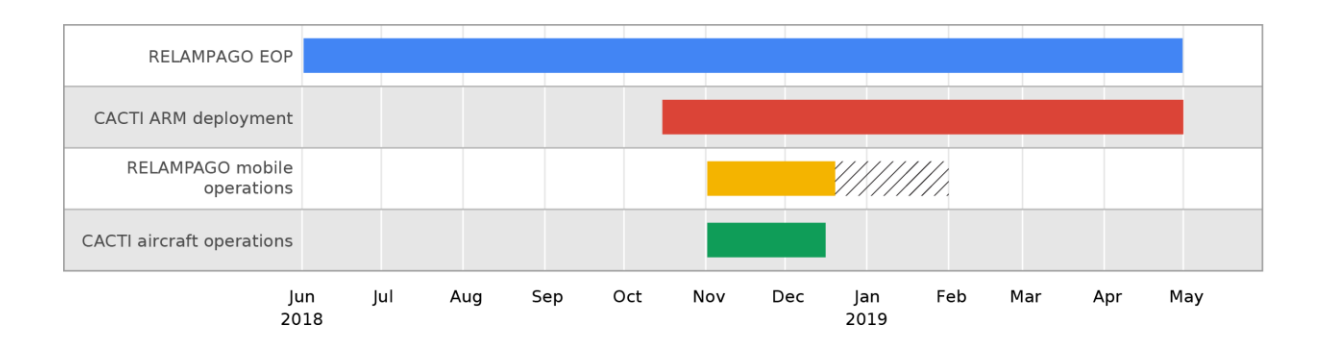


Fig. 2. Timeline of RELAMPAGO-CACTI deployments.

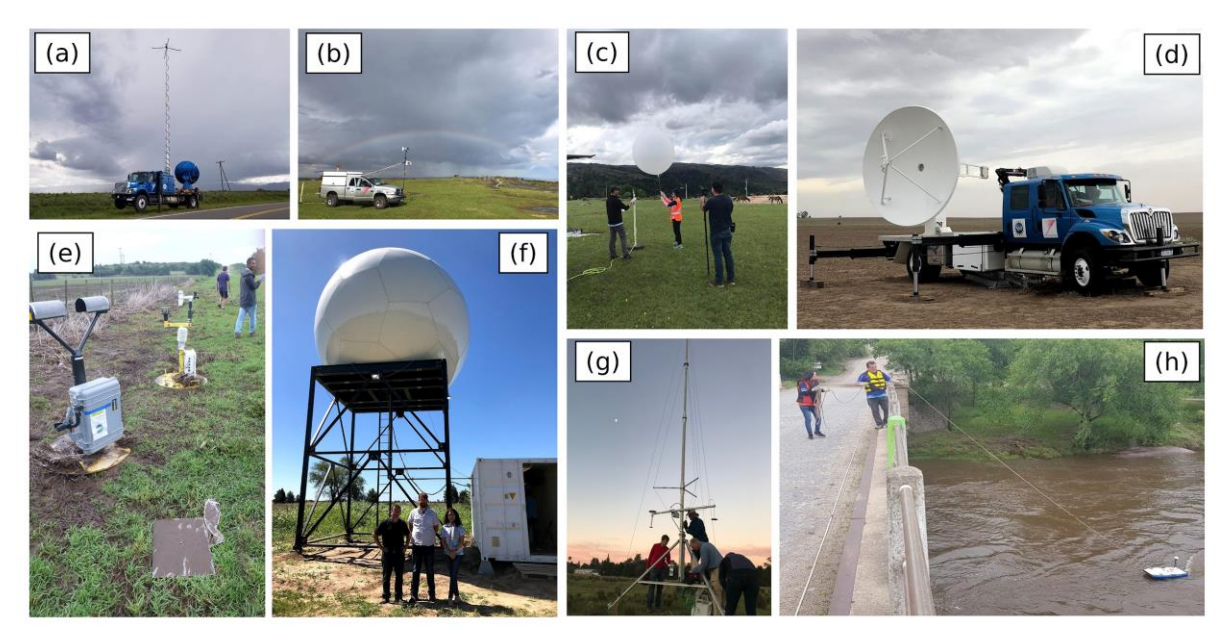


Fig. 3. Photos of selected RELAMPAGO instrumentation: (a) CSWR DOW7 near the SDC, (b) CSWR Scout 2 mesonet vehicle, (c) mobile radiosonde team, (d) COW, (e) Pod and disdrometer, (f) CSU C-Band radar, (g) NCAR EOL ISFS tower installation, (g) Acoustic Doppler Current Profiler.

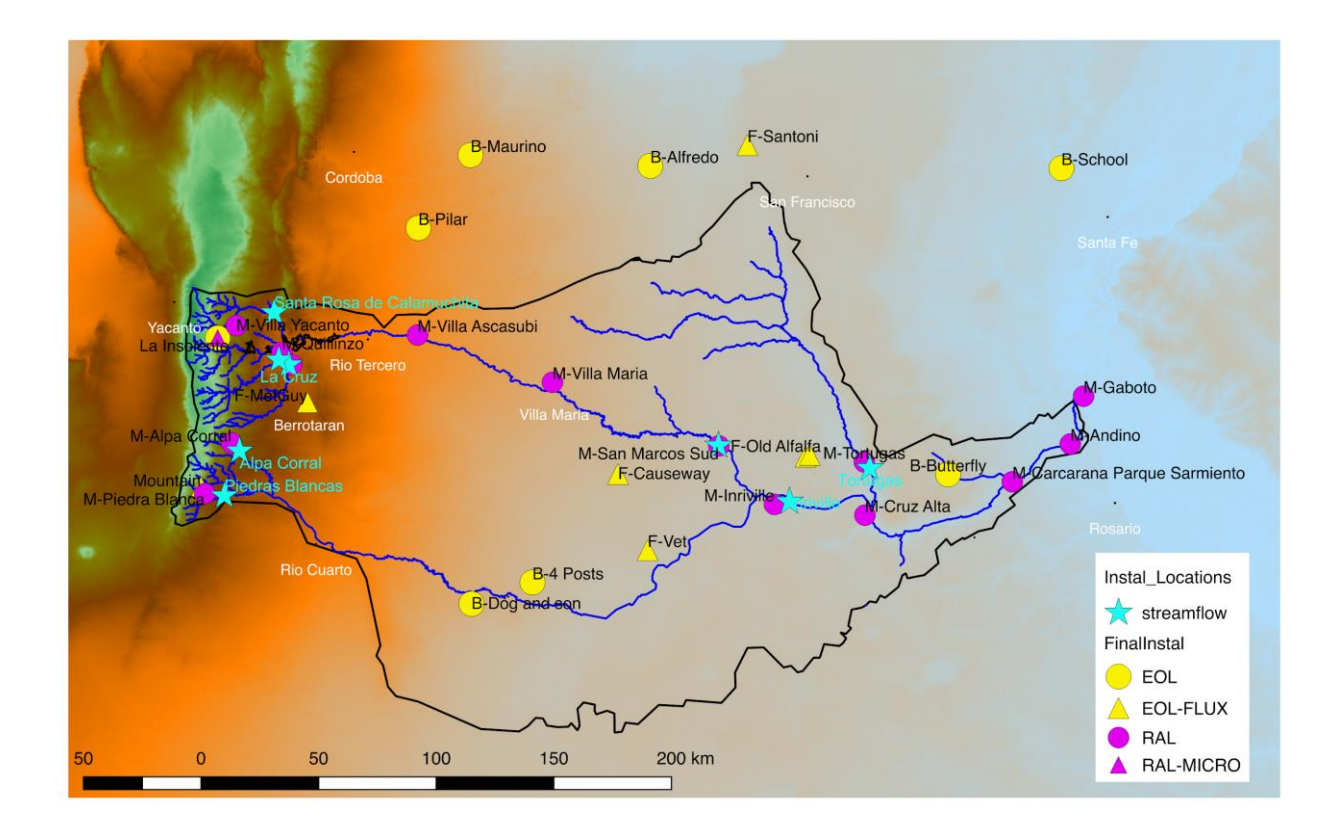


Fig. 4. RELAMPAGO streamflow measurements (cyan stars), NCAR EOL towers (yellow) including the EC towers (triangles), and RAL towers (magenta) including the micro-radars (triangles). The black outline is the Carcarañá river basin, shading indicates topography.

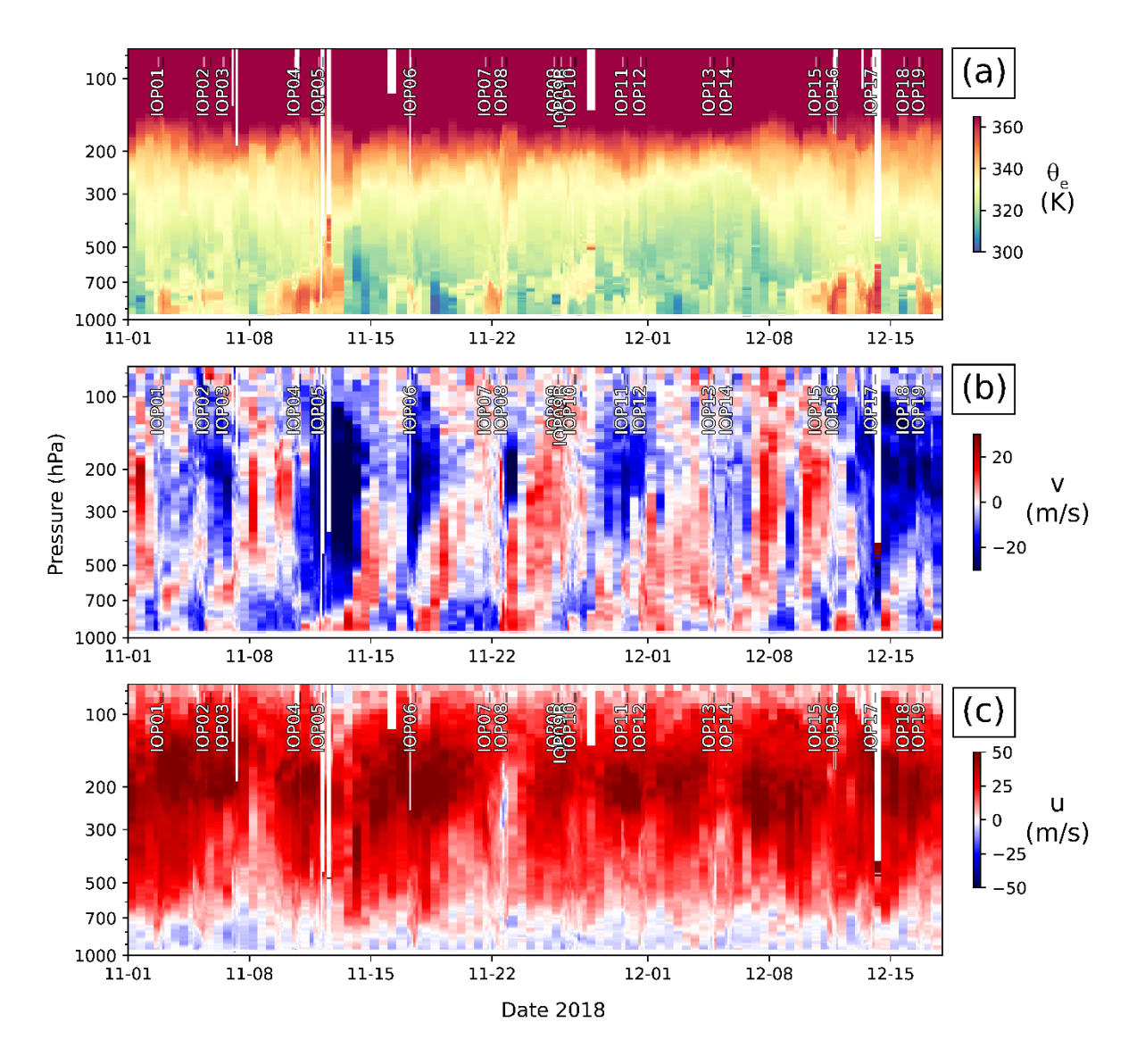


Fig. 5. Sounding-derived time series of (a) equivalent potential temperature (K), (b) meridional wind (m/s), and (c) zonal wind (m/s) from the NCAR 5 hPa interpolated sounding dataset from Córdoba during the RELAMPAGO IOP. RELAMPAGO mission timing is noted in each panel.

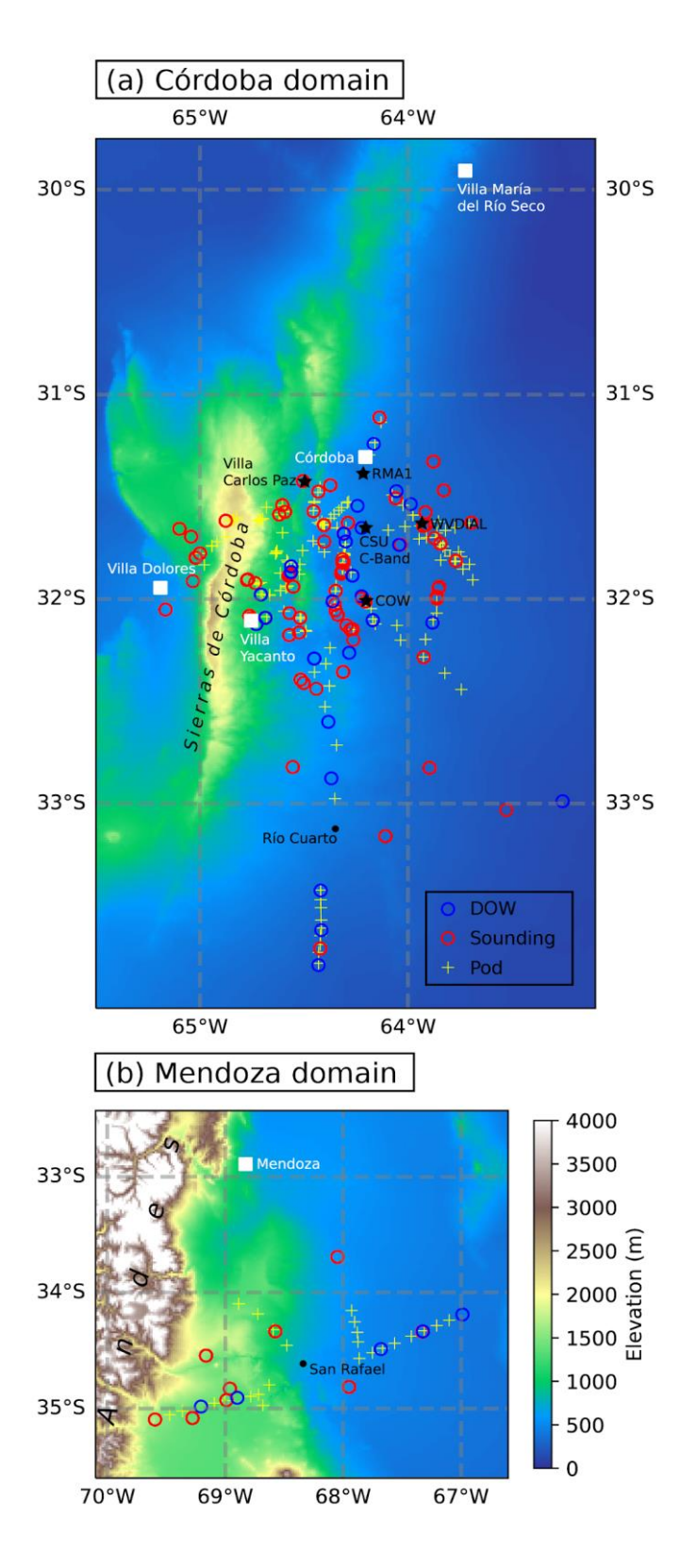


Fig. 6. Map showing fixed sounding assets (white squares), radars and the operations center (black stars) and DOW, sounding, and Pod deployment locations.

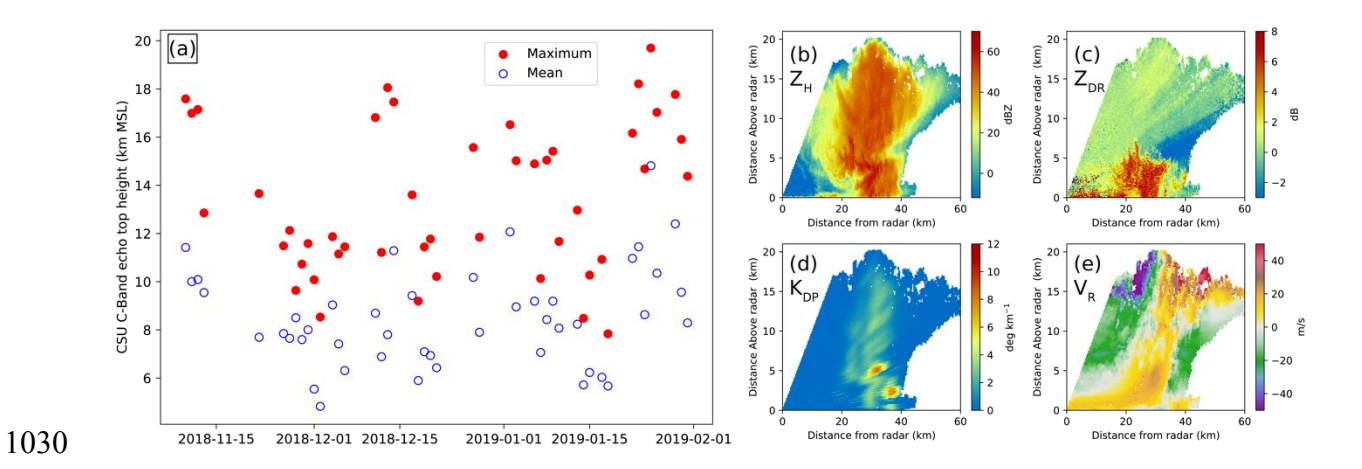


Fig. 7. (a) Daily 18 dBZ echo top height statistics (MSL) from the CSU C-Band radar: daily mean echo top (blue symbols) and maximum echo top (red symbols). From a range height indicator scan at 2034 UTC 25 January 2019 at 257° azimuth: (b) radar reflectivity, (c) differential reflectivity, (d) specific differential phase, (e) radial velocity.

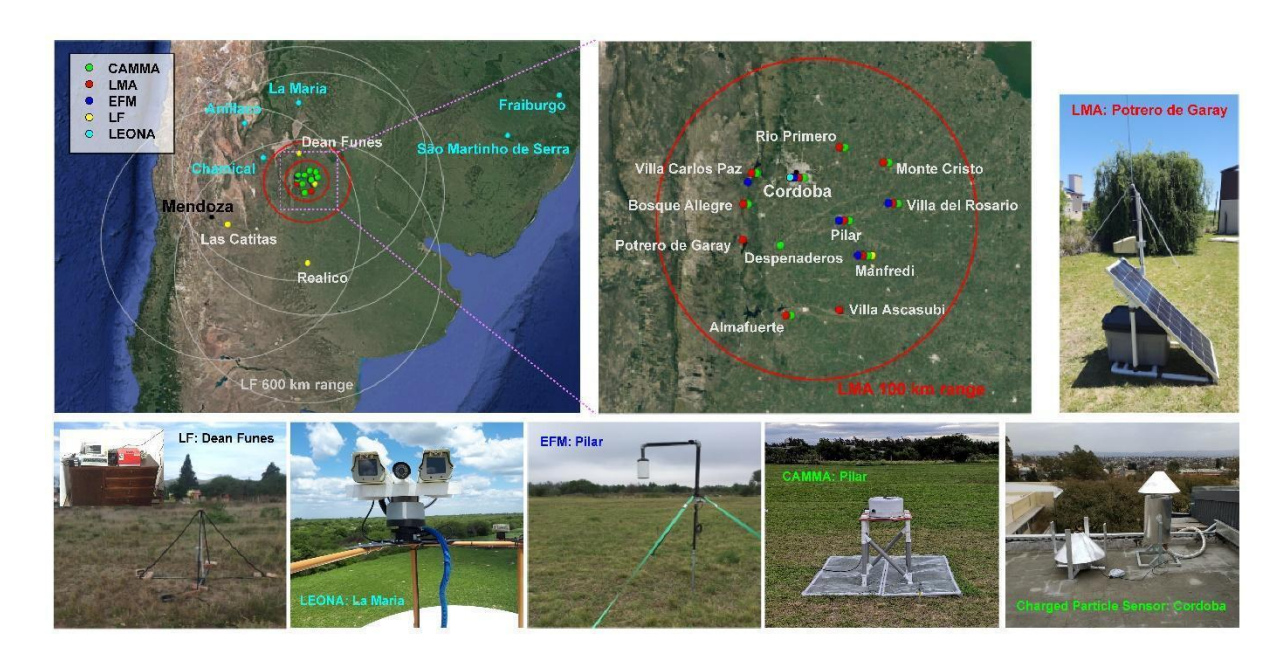


Fig. 8. Maps of the lightning and FAIRIES instrumentation that operated during

RELAMPAGO, and photographs of selected instruments.

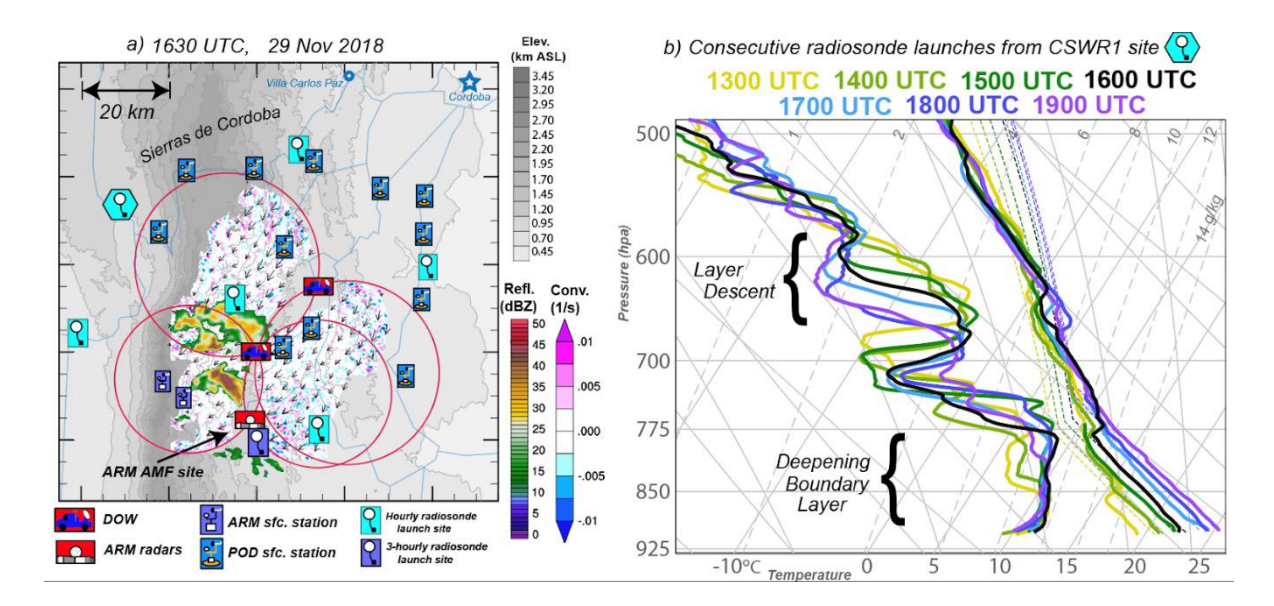
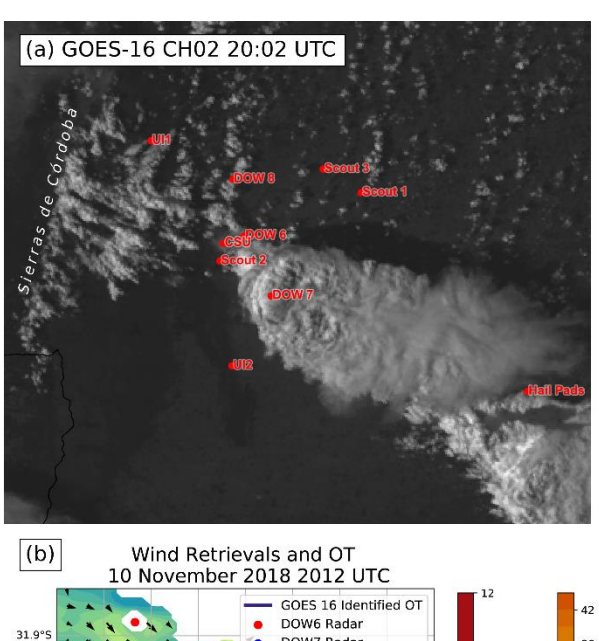


Fig. 9. (a) Deployment map of mobile and fixed assets on 29 Nov 2018, typifying a RELAMPAGO mission targeting terrain-focused CI. Dual-Doppler wind synthesis lobes (red circles), low-level radar reflectivity, and retrieved horizontal flow convergence are overlaid upon topography. (b) Consecutive hourly radiosonde soundings launched from one of the mobile facilities during the deployment. Lifted parcel profiles assume parcels with mean properties of the lowest 100 hPa of the atmosphere.



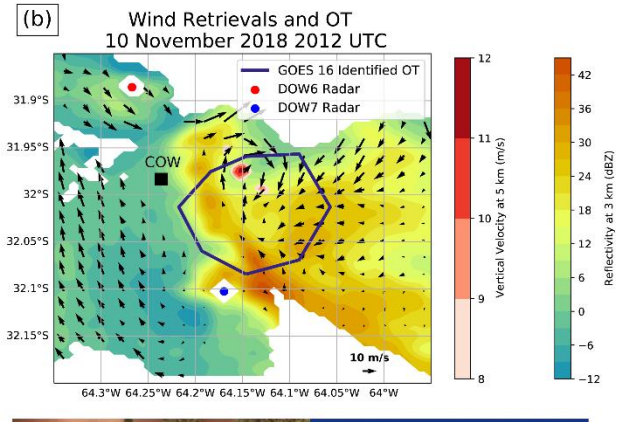




Fig. 10. (a) GOES-16 Channel 2 visible (Red, 0.64 μm) image from 2002 UTC on 10 November along with RELAMPAGO mobile asset locations showing the supercell with overshooting top and above-anvil cirrus plume. (b) DOW6 reflectivity, dual-Doppler synthesis from DOW6 and DOW7, and GOES-16 overshooting top at 20:12 UTC, and the location of the COW radar, (c) hail observation near the COW (left) and COW rear side antenna damage (right).

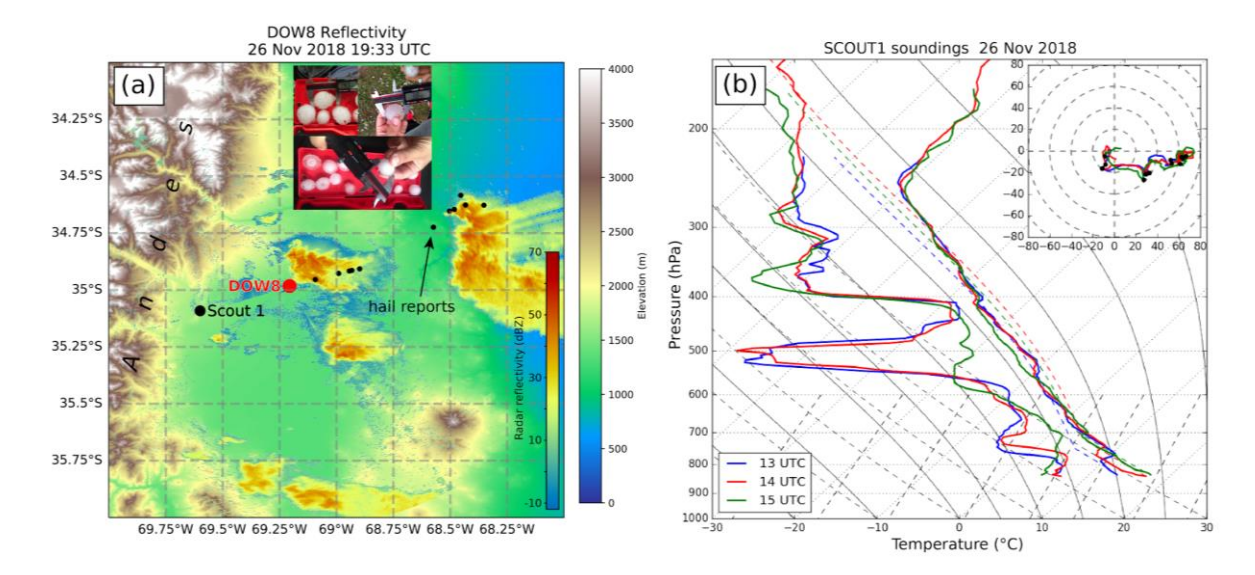


Fig. 11. (a) DOW8 0.9° radar reflectivity from 26 November 2018 at 1933 UTC, topography (shaded), and hail reports from spotters and hail pads (black markers) and SCOUT1 mobile sounding unit (white symbol). (b) Skew-T log p diagram showing temperature and dewpoint (solid lines), and lifted parcel paths (dashed lines) and hodographs (kts) from the 1300, 1400, and 1500 UTC soundings from SCOUT1 on 26 November 2018.

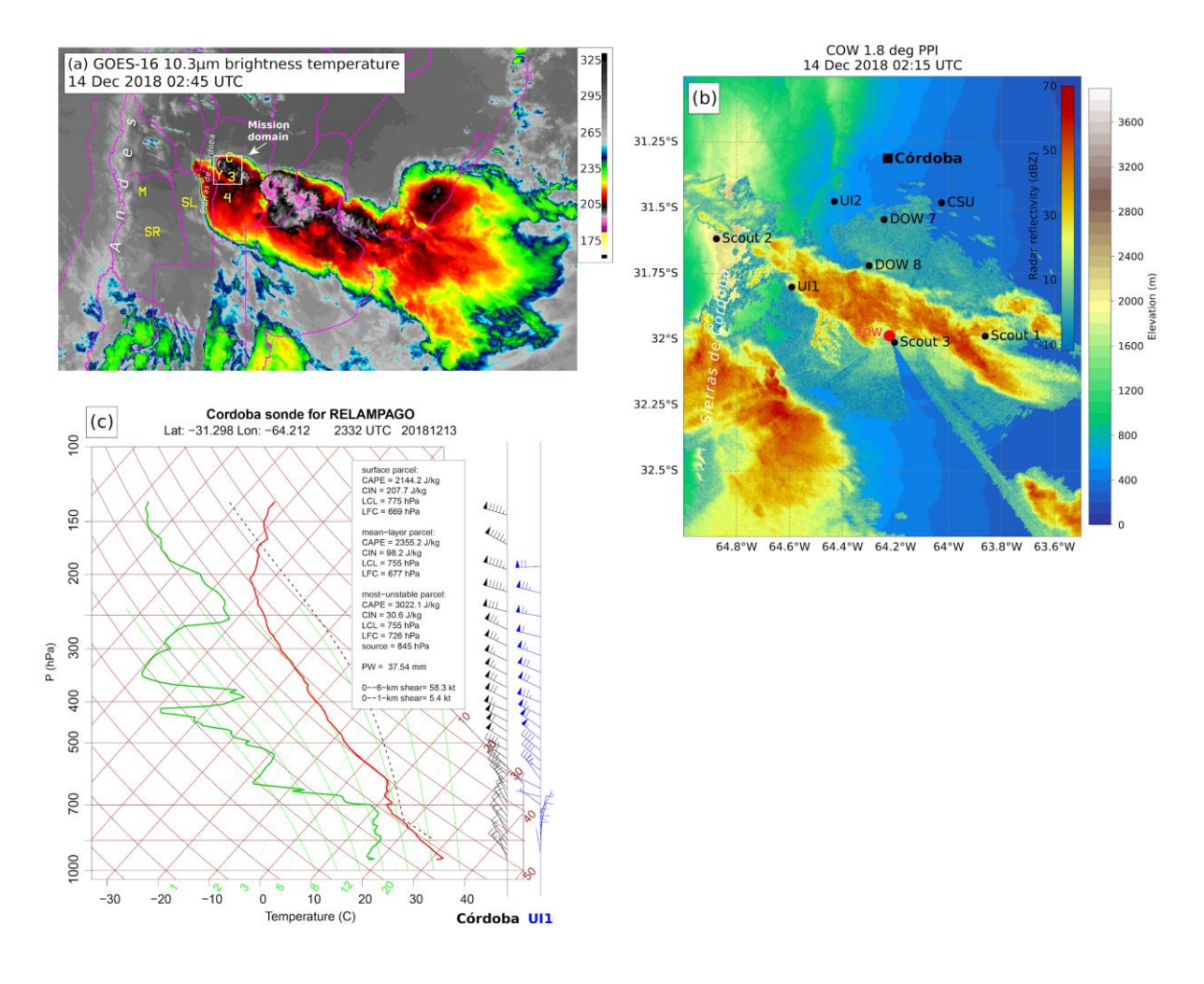


Fig. 12. (a) GOES-16 "clean IR" image showing the IOP14 convective system. The domain shown in (b) is indicated by the white box. (b) COW 1.8° radar reflectivity from 14 December 2018 at 0215 UTC, topography (shaded), and hail reports from spotters and hail pads (black markers) and selected assets (black symbols). (c) Skew-T log p diagram showing temperature and dewpoint (solid lines), and lifted parcel paths (dashed lines) from the 00 UTC 13 December 2018 Córdoba sounding, and winds from the 00 UTC Córdoba (black) and UI1 soundings (blue), full barb is 10 kt.



Fig. 13. Photos from RELAMPAGO education and outreach activities.

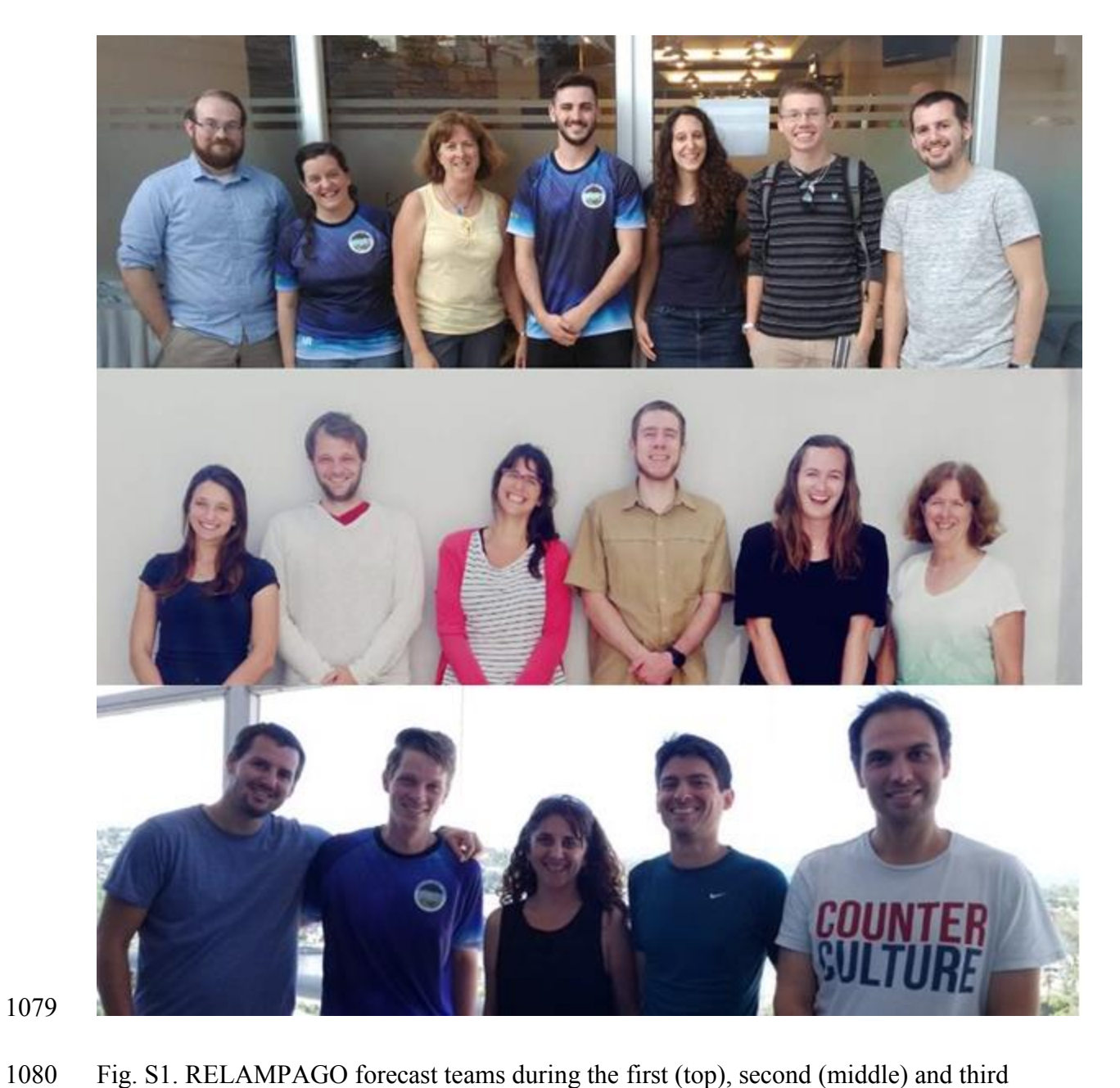


Fig. S1. RELAMPAGO forecast teams during the first (top), second (middle) and third (bottom) parts of the project.



Fig. S2. Group photo of RELAMPAGO mobile teams. (Photo credit: Miguel Ottaviano)